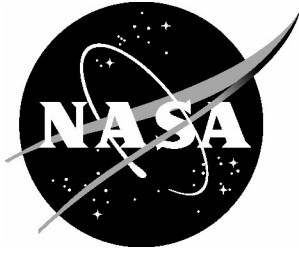


NASA/TM-20250002914



Display Concept for Improved Spacecraft Handling Qualities During Lunar Landing

*Randall E. Bailey, Jason R. Neuhaus, and Lynda J. Kramer
Langley Research Center, Hampton, Virginia*

April 2025

NASA STI Program Report Series

Since its founding, NASA has been dedicated to the advancement of aeronautics and space science. The NASA scientific and technical information (STI) program plays a key part in helping NASA maintain this important role.

The NASA STI program operates under the auspices of the Agency Chief Information Officer. It collects, organizes, provides for archiving, and disseminates NASA's STI. The NASA STI program provides access to the NTRS Registered and its public interface, the NASA Technical Reports Server, thus providing one of the largest collections of aeronautical and space science STI in the world. Results are published in both non-NASA channels and by NASA in the NASA STI Report Series, which includes the following report types:

- **TECHNICAL PUBLICATION.** Reports of completed research or a major significant phase of research that present the results of NASA Programs and include extensive data or theoretical analysis. Includes compilations of significant scientific and technical data and information deemed to be of continuing reference value. NASA counterpart of peer-reviewed formal professional papers but has less stringent limitations on manuscript length and extent of graphic presentations.
- **TECHNICAL MEMORANDUM.** Scientific and technical findings that are preliminary or of specialized interest, e.g., quick release reports, working papers, and bibliographies that contain minimal annotation. Does not contain extensive analysis.
- **CONTRACTOR REPORT.** Scientific and technical findings by NASA-sponsored contractors and grantees.

- **CONFERENCE PUBLICATION.** Collected papers from scientific and technical conferences, symposia, seminars, or other meetings sponsored or co-sponsored by NASA.
- **SPECIAL PUBLICATION.** Scientific, technical, or historical information from NASA programs, projects, and missions, often concerned with subjects having substantial public interest.
- **TECHNICAL TRANSLATION.** English-language translations of foreign scientific and technical material pertinent to NASA's mission.

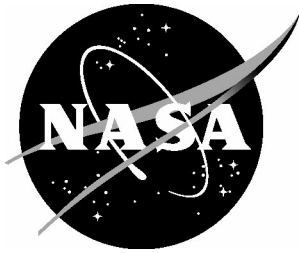
Specialized services also include organizing and publishing research results, distributing specialized research announcements and feeds, providing information desk and personal search support, and enabling data exchange services.

For more information about the NASA STI program, see the following:

- Access the NASA STI program home page at <http://www.sti.nasa.gov>
- Help desk contact information:

<https://www.sti.nasa.gov/sti-contact-form/>
and select the "General" help request type.

NASA/TM-20250002914



Display Concept for Improved Spacecraft Handling Qualities During Lunar Landing

*Randall E. Bailey, Jason R. Neuhaus, and Lynda J. Kramer
Langley Research Center, Hampton, Virginia*

National Aeronautics and
Space Administration

Langley Research Center
Hampton, Virginia 23681-2199

April 2025

Acknowledgments

This work began under the Constellation Program and has been improved upon to match the needs of the Artemis Program, Human Landing Systems (HLS) Project. The authors wish to acknowledge the support of the Artemis Program, HLS Crew Compartment (CrewCo) office and specifically, the Crewed HLS Interfaces for Piloting (CHIP) Working Group, led by Mr. Everett Bolduc and Mr. Steve Carothers.

The use of trademarks or names of manufacturers in this report is for accurate reporting and does not constitute an official endorsement, either expressed or implied, of such products or manufacturers by the National Aeronautics and Space Administration.

Available from:

NASA STI Program / Mail Stop 050
NASA Langley Research Center
Hampton, VA 23681-2199

Table of Contents

1.	INTRODUCTION.....	7
2.	BACKGROUND	8
2.1.	APOLLO HANDLING QUALITIES CRITERION	8
2.2.	REVISIT OF LUNAR LANDING HANDLING QUALITIES CRITERION	10
2.3.	DISPLAY CONCEPT – HOVER CUE.....	12
3.	DISPLAY CONCEPT.....	13
3.1.	HOVER CUE CONCEPT	13
3.2.	INTEGRATED SYMBOLOGY SET	14
3.3.	HOVER CUE DESIGN CONCEPT	16
3.4.	DESIGN	18
3.5.	VELOCITY VECTOR PORTRAYAL	19
4.	DERIVATION OF HOVER CUE CONTROL LAWS.....	20
4.1.	ADAPTATION FOR RATE COMMAND, ATTITUDE HOLD (RCAH).....	20
4.2.	RESULTS – HOVER CUE COMPARED TO EXPLICIT GUIDANCE.....	21
4.3.	ADAPTATION FOR ATTITUDE-COMMAND, VELOCITY HOLD (ACVH):	22
4.4.	HOVER CUE WITH ACVH AND RCAH	23
5.	PRACTICAL APPLICATION EXPERIENCE	25
5.1.	NON-ATMOSPHERIC FLIGHT CONSIDERATIONS.....	25
5.2.	BANDWIDTH SELECTION	25
5.3.	ND RANGE / RANGE CONTROL.....	25
5.4.	INSTANTANEOUS CENTER-OF-ROTATION COMPENSATION	26
5.5.	RCAH AND ACVH CHARACTERISTIC VALUES	28
5.5.1.	RCAH K VALUES.....	28
5.5.2.	RCAH τ VALUES	28
5.5.3.	ACVH K VALUES.....	31
5.5.4.	ACVH ω AND ζ VALUES	31
6.	IMPROVEMENTS	33
6.1.	HOVER CUE VS. MODIFIED ACCELERATION BALL.....	33
6.2.	LARGE ATTITUDE OPERATIONS	34
6.2.1.	REMOVE SMALL ANGLE APPROXIMATIONS	34
6.2.2.	LIMITERS.....	34
6.3.	IMPROVEMENT SUMMARY	35
7.	CONCLUDING REMARKS.....	36
	REFERENCES	37
	APPENDIX A: ACVH HOVER CUE DERIVATION.....	39

List of Figures

FIGURE 1: LUNAR LANDING HQ CRITERION FROM APOLLO (FIGURE 9 FROM REF. 1).....	9
FIGURE 2: TRANSLATION BY ROTATION WITH RCS ATTITUDE CONTROL	9
FIGURE 3: APOLLO LUNAR MODULE COMPARED TO REF. 1	11
FIGURE 4: HEAD-DOWN DISPLAYS FROM REF. 12.....	11
FIGURE 5: HOVER CUE CONCEPT	13
FIGURE 6: NAVIGATION DISPLAY WITH HOVER CUE INTEGRATED SYMBOLOGY SET	15
FIGURE 7: IDEAL HOVER CUE TASK SCHEMATIC DIAGRAM.....	16
FIGURE 8: ROOT LOCUS FOR IDEAL HOVER CUE LOOP CLOSURE	18
FIGURE 9: COMPARISON OF ω_0 VARIATIONS	18
FIGURE 10: GEOMETRY OF HOVER CUE DRAWING IN DISPLAY UNITS (DUs).....	19
FIGURE 11: TRANSLATION BY ROTATION USING ENGINE GIMBALLING.....	26
FIGURE 12: EXAMPLE RCAH-RCS TIME RESPONSE FOR ONE-THIRD STICK INPUT.....	30
FIGURE 13: EXAMPLE RCAH-RCS TIME RESPONSE FOR TWO-THIRDS STICK INPUT	31

Nomenclature

ACVH	Attitude Command, Velocity Hold
CP	Control Power
DU	Display Unit
GRM	Government Reference Model
HH	Hover Hold
HLS	Human Landing System
HQR	Handling Qualities Rating
ICR	Instantaneous Center-of-Rotation
IPC	Incremental Position Control
LIDAR	Light Detection and Ranging
LM	Lunar Module
LT	Landing Target
NASA	National Aeronautics and Space Administration
ND	Navigation Display
OTW	Out-the-Window
PFD	Primary Flight Display
PIO	Pilot-Induced Oscillations
RCAH	Rate Command, Attitude Hold
RCS	Reaction Control System
SHaQ	Spacecraft Handling Qualities
TM	Technical Memorandum
TVC	Thrust Vectoring Control
VMS	Vertical Motion Simulator

1. Introduction

During Apollo, the commander relied on the out-the-window (OTW) view during the final stages of the approach and landing for hazard avoidance and vehicle control since this was the primary, if not the sole source, of information available to them to successfully accomplish the task (Ref. 1).

Apollo technology could not provide the pilot with electronic displays of sensor and guidance information to direct them to suitable, hazard-free landing sites. Significant research was conducted to develop the Apollo flight control system design requirements for good lunar landing handling qualities for a thrust-vectoring vehicle flying under the 1/6th gravity of the moon while only using the pilot's natural vision, OTW (Ref. 2).

To further ensure that the commander succeeded in this mission, the Apollo program made critical decisions, including:

- A “pitch-up” maneuver in the final approach descent phase and a judiciously-designed window configuration gave the flight crew approximately 2 minutes of OTW viewing of the planned landing site. The pitch-up sacrificed fuel usage by rotating the vehicle to a near vertical orientation, allowing the crew to identify and fly to a suitable landing site (e.g., free of rocks and craters, acceptable terrain slope) through a window which provided ~70° nose-low visibility. (Ref. 3)
- Selection of landing sites and mission times around lighting conditions that would create optimal viewing OTW. (Ref. 4 and 5)
- Special purpose vehicles constructed to develop control law design requirements and to train the crews – the Lunar Landing Research Vehicle and the Lunar Landing Training Vehicles, respectively. (Ref. 6)

These constraints placed by the design of the Lunar Module (LM) window for crew visibility and landing trajectory were “a major problem.” (Ref. 3)

NASA's Artemis campaign will return humans to the Moon for scientific discovery, technology advancement, and to learn how to live and work on another world. Building on Apollo, NASA will return Astronauts to the surface of the Moon using innovative technologies and lunar landers designed and built by commercial partners. The mission design constraints of Apollo for OTW visibility will be significantly relaxed. The Artemis Human Landing System (HLS) project is planning missions to the scientifically-rich areas near the South Pole of the Moon for which the OTW view is extremely compromised (Ref. 7). Trajectories to the landing site will be tailored toward fuel-optimal with little, if any, “pitch-up.” (Ref. 8)

Fortunately, the sensing and display technologies of today may alleviate the problems caused by relaxation of the Apollo design constraints for lunar landing manual control. In the following, a display concept for improved Spacecraft Handling Qualities (SHaQ) during manual control of the final approach and lunar landing is presented.

2. Background

The return of humans to the moon under Artemis will be achieved by a combination of automatic and manual control, where automatic control is likely the primary mode of operation but manual control provides “the crew the ability to take control of the spacecraft, especially during critical phases, if there are issues with the automated system (failures or unexpected performance) to: (1) protect crew survivability; and, (2) enable mission success.” (Ref. 9)

These manual control capabilities must also provide Level 1 handling qualities as per paragraph 4.5.2 of NASA Technical Requirements for Human-Rating (NASA-STD-8719.29, dated 2023-12-11):

The crewed spacecraft shall exhibit Level 1 handling qualities (Handling Qualities Rating (HQR) 1, 2 and 3), as defined by the Cooper-Harper Rating Scale, during manual control of the spacecraft's flight path and attitude for crew manual control events when the vehicle has not had failures which result in degraded flight control.

2.1. Apollo Handling Qualities Criterion

The Apollo program extensively studied manual control during lunar landing, tackling the problem of controlling a thrust-vectoring vehicle, operating in 1/6th Earth's gravity without an atmosphere. Fixed-base simulation studies scoped out the parameter space and developed initial requirements. (Ref. 1 and 3)

An in-flight simulation vehicle - the Lunar Landing Research Vehicle - was critical in the manual control requirements development as only it could adequately simulate the visual and motion cues with realistic trajectories for this task. (Ref. 10)

The primary criterion to emerge is shown in Figure 1, which defines acceptable and satisfactory attitude control characteristics for pilot control of the longitudinal and lateral velocities of the spacecraft; that is, to achieve a hover (zero translational velocity) for the lunar approach and landing task. This criterion is defined by the maximum steady-state rate response and the rate response time constant (i.e., the time to reach the maximum steady-state rate response). Although it is also critical for satisfactory completion of the task, this work does not capture the requirements for vertical (height) control. The practical manifestation of these attitude control requirements and design constraints to meet the challenge of the lunar landing are highlighted in Reference 11.

The Apollo criterion of Cheatham and Hackler (Figure 1) is defined using a maximum rate command and a “time constant” parameter where the time constant is the time to reach the maximum rate. For a Rate Command, Attitude Hold (RCAH) lunar landing vehicle, the criterion essentially becomes: 1) the chosen maximum rate command provided to the pilot (i.e., the y-axis “Maximum Rate Command”), and 2) the Maximum Rate Command (deg/sec) divided by the rotational control power (deg/sec²) of the vehicle (i.e., the “Time Constant”).

The criterion assumes translation by rotation, effected by Reaction Control System (RCS) jets as illustrated in Figure 2 where:

T is Thrust

cm is the center-of-mass

x is the forward direction of flight

θ is the vehicle pitch attitude (in “aircraft” coordinate frame i.e., where +X is forward, +Y is right, and +Z is down)

The maximum rotational acceleration authority – the Control Power (CP) – is approximately the RCS jet thruster size (T_{RCS}), multiplied by the number of RCS jets used for control about a given axis and their moment arm divided by the rotational inertia. The thruster firings of the RCS jets create attitude changes which effectively translate the vehicle. Any attitude different than zero creates a translational acceleration relative to the lunar surface.

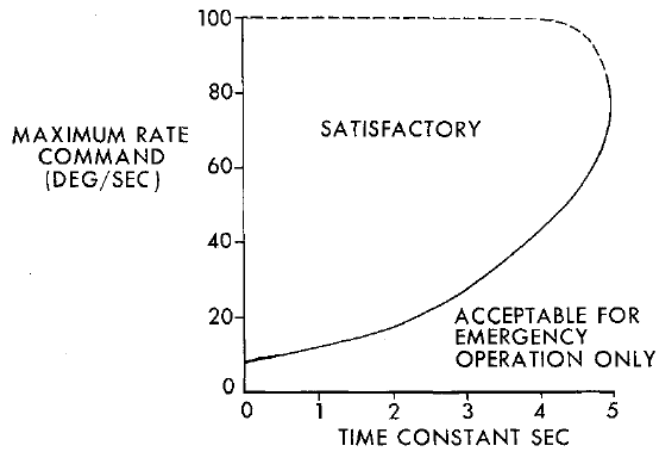


Figure 1: Lunar Landing HQ Criterion from Apollo (Figure 9 from Ref. 1)

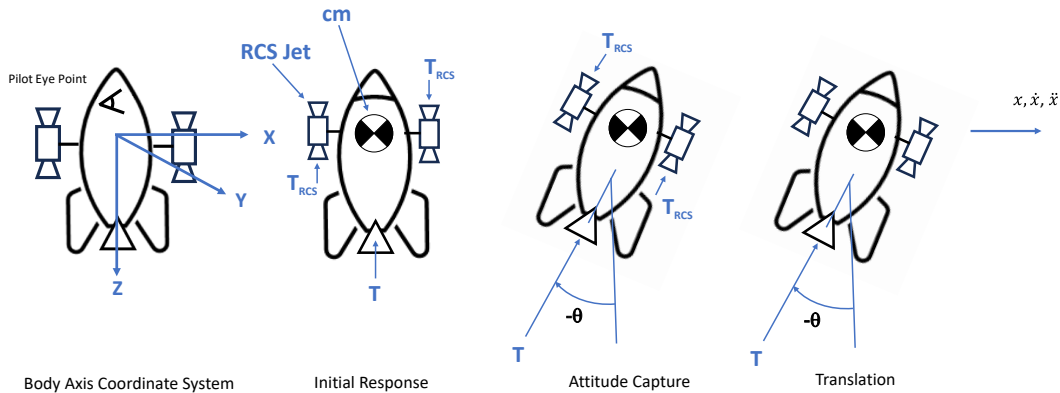


Figure 2: Translation by Rotation with RCS Attitude Control

For the Apollo LM, nominally, only two RCS jets were fired to conserve RCS propellant but for circumstances that dictated higher rotational control (e.g., excessive rate error in the RCAH control law), four jets were used.

2.2. Revisit of Lunar Landing Handling Qualities Criterion

Under NASA's Constellation program, a return to the moon was again contemplated. The planned return reinvigorated research into spacecraft handling qualities requirements.

NASA Ames conducted a Vertical Motion Simulator (VMS) test evaluating the validity of the Cheatham-Hackler criterion as well as other lunar lander design issues.

In this evaluation (Ref. 12), an Apollo LM-type vehicle was simulated with variations in control power starting at the nominal Apollo design values (between the 8.6 deg/sec² four-RCS jet and 4.3 deg/sec² two-RCS jet control power, depending upon pitch / roll inputs and attitude error magnitude) and then reducing control power to 10% of that value. A 20 deg/sec maximum roll and pitch rate command was used in the RCAH control law. The final approach "glideslope" for the nominal trajectories was approximately 15 deg, mirroring the initial Apollo lunar landings. The nominal configuration compared to Cheatham-Hackler criterion is shown in Figure 3.

Unlike Apollo, the pilot was provided with electronic displays in addition to the OTW view (Figure 4), especially:

- A Navigation Display (ND) showing a god's-eye view of the location of the landing target, ownship position, and translational velocities.
- Explicit pitch and roll guidance with rate-of-descent commands to follow a path to the hover transition point, hover, and then vertical descent to landing. The guidance was shown on the head-down Primary Flight Display (PFD).

The experimental data showed that the nominal Apollo-type configuration was Level 1 (Cooper-Harper pilot ratings, Ref. 13, of 2 and 3), with guidance, generally correlating with Cheatham-Hackler. Handling qualities degraded as the control power was reduced.

Pre-test work showed that, without explicit guidance, the evaluation pilots could not reliably complete the lunar landing task that included a lateral offset. (The lateral offset task was added to increase the piloting task demands.) The simulated OTW view was of significantly less fidelity than the real-world and the field-of-view was not nearly as large as the Apollo 70 deg nose-low visibility. Only a straight-in task could be flown without guidance.

For the no-offset task and without guidance, the nominal configuration exhibited Level 1 handling qualities, matching the Cheatham-Hackler criterion.

With explicit pitch/roll guidance commands (with an offset task), the nominal configuration also exhibited Level 1 handling qualities, matching the Cheatham-Hackler criterion.

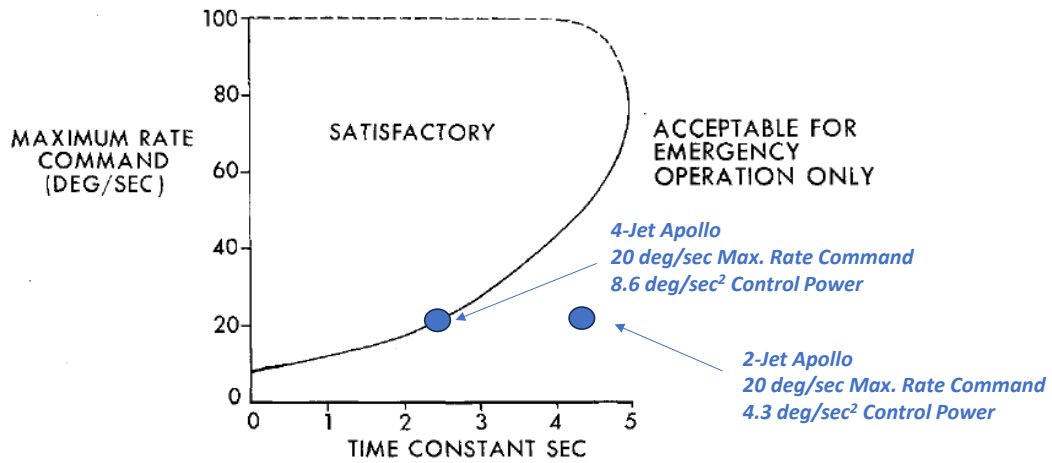


Figure 3: Apollo Lunar Module Compared to Ref. 1

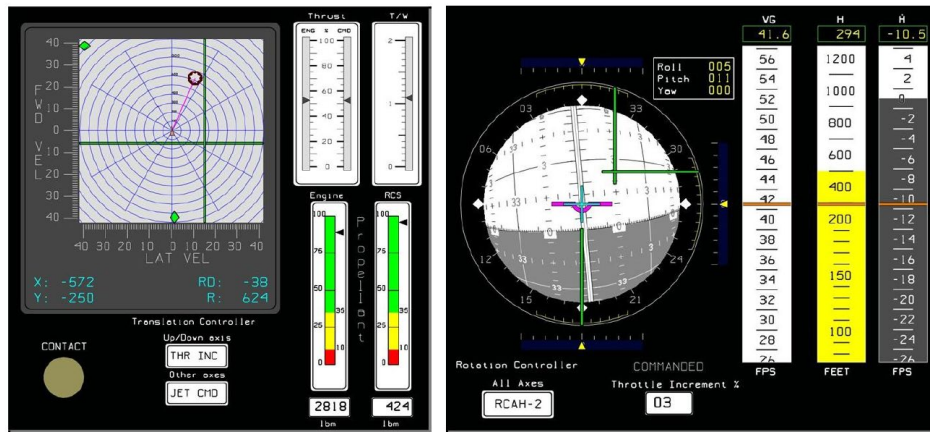


Figure 4: Head-Down Displays from Ref. 12

The results suggest that the Cheatham-Hackler criterion is appropriate for a straight-in landing task without guidance using sufficient OTW visual cues. The pilots were not able to satisfactorily achieve desired performance flying an offset approach without guidance for configurations that Cheatham-Hacker would suggest are “acceptable for emergency operation only.”

If guidance is used, Level 1 handling qualities ratings in accordance with Cooper-Harper rating scale were given for the offset landing task for the nominal configuration.

The pilot comments and ratings suggested that the lunar landing manual control task, with redesignation (lateral offset) could be achieved for vehicles with less control power than required by Cheatham-Hackler by using today’s cockpit technologies.

2.3. Display Concept – Hover Cue

In this VMS test, however, the pilot's attention was shown to be extensively focused head-down following the explicit pitch/roll command guidance (described in Ref. 12). The pilot's attention on the explicit command guidance increased as the control power was reduced. The pilots found that the display of command guidance was still effective, but they had little time to attend to the out-the-window view or other task demands. When presented with sluggish attitude control, the pilots found it difficult to track the explicit pitch/roll guidance to stay on-path to the planned touchdown location and if they got behind the guidance, they couldn't "catch up" because of the sluggish attitude control response. This issue is compounded by the abstract nature of the flight director needles which don't intuitively convey to the pilot a rationale for the magnitude and direction of the command guidance movements.

These results spurred the development of a display concept to aid manual control of spacecraft. The primary objective was to decouple the manual piloting task from the flight guidance system. With explicit command guidance, the pilot is reliant on and may need to interact with the flight guidance system to redesignate the landing target – a possibly time-intensive task that may be performed at low altitudes and possibly with no guarantee of a trajectory solution. The display concept was also designed for improved handling qualities compared to explicit pitch / roll command guidance systems (e.g., better task performance, lower pilot workload).

The proposed solution was a new control/display element in the form of a hover cue. The spacecraft hover cue closely follows from Ref. 14 with adaptation for a non-atmospheric flying vehicle.

The motivation for this display element is that, if successful, a hover cue would be ideally suited for a manual controlled re-designated landing task, especially when coupled with a head-up display or head-worn display projecting this cue against conformal imagery or the actual lunar terrain. The hover cue may also be displayed head-down on the ND.

Unlike the explicit pitch / roll guidance, the hover cue is a situation information display element for the pilot. The cue is not an abstract display of commands to follow a planned trajectory, but is more intuitively associated with the pilot's control inputs and the task of coming to a hover over the landing target. The pilot sees in the hover cue, a visual representation of the effect of their control inputs on the translational control task. The hover cue is not part of the flight guidance system but is an aid for manual control analogous to a head-up display, flight path marker.

3. Display Concept

The hover cue algorithm emerges from rotorcraft work (Ref. 14) with adaptation for a non-atmospheric flying vehicle as described in the following.

The hover cue is, in essence, a piloting aid showing the continuously-computed hover position on a head-up or head-down display with inclusion of pilot control actions to achieve this hover position.

3.1. Hover Cue Concept

The hover cue is part of an integrated symbology set, including the ownship position symbol, velocity vector, and conformal landing zone designator and/or underlay map. (The term conformal is used herein to mean that the displayed elements are aligned and scaled together.)

The hover cue is mechanized as a “fly-to” symbology element where the positioning and dynamics of the cue provides situational information for the pilot to smoothly approach a desired hover point and achieve zero horizontal velocity (i.e., a hover condition). Vertical control is also a critical component of a successful spacecraft approach and landing task but it is not addressed herein.

The pilot’s task is to use the pitch and roll inceptor to place the hover cue over the desired landing site and maintain that position (i.e., “put the ball on the landing target”). It is not a “set-and-forget” display element; to maintain the position of the hover cue over the desired hover point requires continual pilot input.

The schematic diagram in Figure 5 illustrates the hover cue concept. The task objective is to translate the vehicle to a desired position (x_c). The error (x_e) between the desired and present vehicle “ownship” position (x) is shown on a display (using a display scale factor, K_x) and depicts the displacement of the ownship from the desired landing target (ΔLT). The pilot manipulates the control inceptor (δ) - closing the loop on the vehicle dynamics to hold the position of the hover cue, A_x , over the displayed landing target (ΔLT).

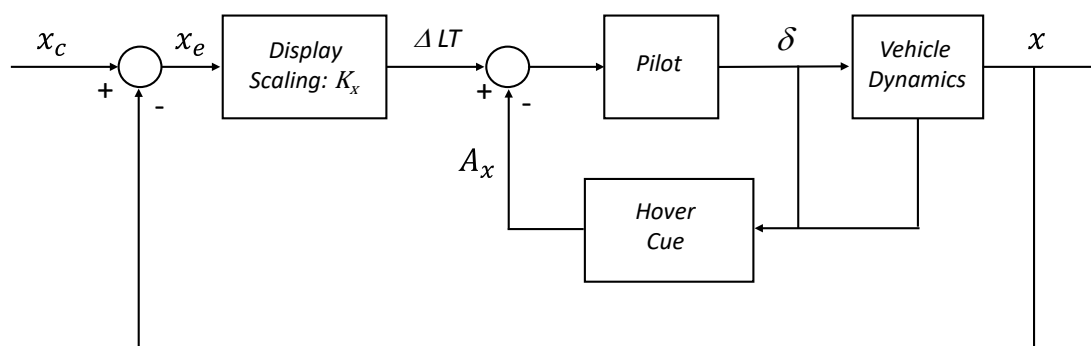


Figure 5: Hover Cue Concept

The hover cue is designed to provide the pilot with visual information aiding this manual control operation for desirable translation and hover control handling qualities as described in Section 3.3.

The control logic is that a nose-down rotational hand controller (inceptor) input from the pilot moves the hover cue downrange or “up” on the display and a nose-up input moves the hover cue uprange or “down” on the display. (A left rotational hand controller input moves the hover cue left on the display, etc.)

3.2. Integrated Symbolology Set

The integrated symbolology set elements, including the hover cue, are shown in Figure 6 and are described as follows using a ND as the example display device:

- **Ownship Symbol:** This symbol corresponds to the vehicle position; it is positioned in a fixed location on the display. The example in Figure 6 shows a quarter-format ownship position that emphasizes information in front of the vehicle. A centered position of the ownship symbol can be used as well providing 360 degree awareness around ownship. Either display concept is viable. The specific implementation is vehicle and task dependent.
- **Range Scale:** The integrated symbolology set elements are conformally drawn with respect to each other. In the case of a ND implementation such as Figure 6, the pilot is informed of the relationship between the displayed elements and the real-world by the range scale. The range scale of “25 m” in Figure 6 indicates that symbology drawn on the first dotted semi-circle from the ownship symbol are 25 m from the ownship. The second dotted semi-circle is twice as far, e.g. 50 m, from the ownship symbol. The landing target is approximately 17 m in front of ownship.
- **Landing Target and/or conformal underlay map:** The pilot controls the hover cue to position it over the desired hover point. This hover point may be any point on a conformal underlay image but is typically a conformal symbolic landing target identifier (e.g., the magenta-colored “doghouse” symbol). In Figure 6, the underlay image is a hazard map with areas of green, yellow, orange, and red indicating a hazard level. An underlay image can be any imagery (e.g., camera image, hazard map, synthetic vision view), as long as it is conformal to the integrated symbolology set.
- **Velocity Vector:** The velocity vector provides a graphical depiction of the vehicle’s velocity (magnitude and direction).
- **Hover Cue:** The hover cue is a graphical representation of where the vehicle will reach a zero translational velocity with respect to the conformal underlay image and/or landing target symbol. The pilot uses the pitch and roll inceptors to place the hover cue and hold its position over the desired conformal map point/landing target (i.e., “put the ball on the landing target and hold it there”).

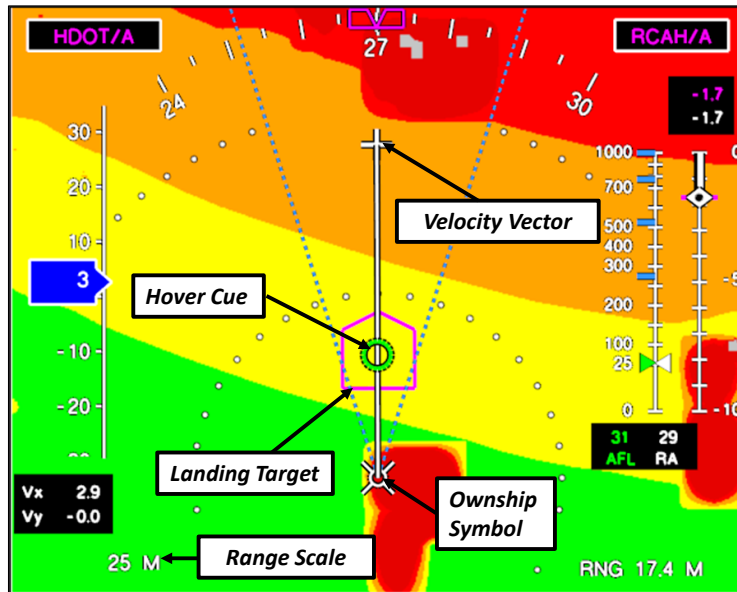


Figure 6: Navigation Display with Hover Cue Integrated Symbology Set

During manual flight operations, the pilot controls the hover cue position. The hover cue is not typically stationary, it will continue to move unless pilot inputs are made to hold its position.

The hover cue, ownship, and the velocity vector provide the pilot with additional cueing:

- When the hover cue and the tip of the velocity vector (the “plus” sign) are coincident, ownship is holding a constant velocity.
- When the hover cue is otherwise positioned away from the “plus” sign, the ownship and velocity vector will move towards the hover cue.
- When the hover cue is placed on top of the ownship symbol, the vehicle will slow to a stop at or near the ownship position.

The hover cue during manual control, in effect, leads the velocity vector and the ownship – that is, the tip of the velocity vector (i.e., the “plus” sign) and the ownship symbol will follow the hover cue symbol until they all reach the same position in a stationary hover.

When the velocity becomes small, the velocity vector line that emanates from the ownship symbol is typically replaced by “cross-hairs” symbology to show the pilot the incremental forward and lateral velocity since it is otherwise very cluttered and difficult to see when the hover cue, the ownship symbol, and the velocity vector converge.

Additional information such as ground speed, altitude, and descent rate is shown on the ND for situation and task awareness as necessary and appropriate to the operation.

3.3. Hover Cue Design Concept

In the design of the hover cue dynamics, it has been assumed that three coincident real-axis roots between the stick position and vehicle velocity produce desirable dynamics (Ref. 14 and 15). Other means of mechanizing the hover cue, such as described in Reference 16, have not been explored at this time since the three coincident root approach has produced excellent results to date.

The positioning of the hover cue following this assumption and, in the ideal case, where the pilot controls the vehicle by following the hover cue perfectly is shown schematically in Figure 7.

- The vehicle needs to translate to a commanded position (x_c).
- The difference between the actual (x) and commanded position (x_c) creates a position error (x_e). Ideally, the pilot will move the inceptor to place the hover cue position (A_x) on top of the displayed landing target (x_e).
- This position error is scaled by the value K_x which is the display mapping parameter. The value of K_x corresponds to the range scale of the ND (or whatever device is being used for the hover cue). K_x is in display units (DUs) per position units (i.e., ND range scale). For example, assuming K_x is in pixels per meter, then a position 25 meters in front of ownship is drawn in DUs of 100 pixels from the ownship symbol, the value of $K_x = 100 \text{ pixels}/25 \text{ m} = 4.0 \text{ pixels}/\text{meter}$.
- Holding the hover cue (A_x) to null the position error (x_e) will, by design of the hover cue, lead the vehicle velocity to follow the “ideal” 3rd order response as defined in Figure 7.

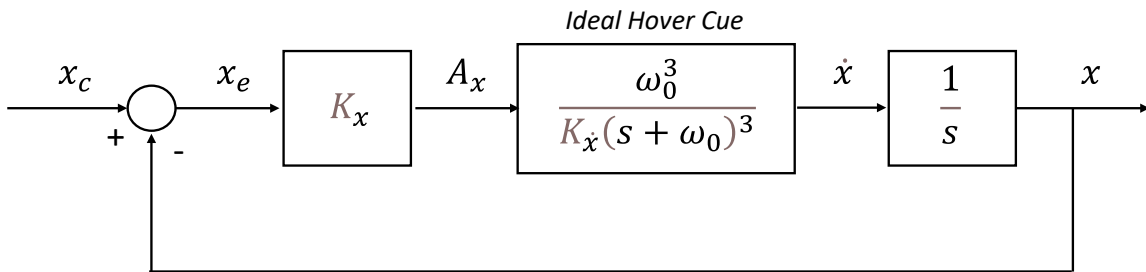


Figure 7: Ideal Hover Cue Task Schematic Diagram

The longitudinal position of the hover cue, A_x , is derived in the following. The lateral position, A_y , is directly analogous, but not shown in this report for brevity.

From this design, the vehicle velocity response for the ideal hover cue is:

$$\frac{\dot{x}}{A_x} = \frac{\omega_0^3}{K_x(s + \omega_0)^3}$$

Rearranging this equation provides the design basis of the hover cue position (A_x):

$$A_x = \frac{\dot{x}K_{\dot{x}}(s+\omega_0)^3}{\omega_0^3} \quad Eqn (1)$$

Where

$K_{\dot{x}}$ is the hover cue scaling, in Display Units (DU) per velocity (distance per sec).

A_x is the position of the hover cue in DUs from the ownship position

ω_0 is a bandwidth parameter, rad/sec

\dot{x} is the body-axis forward velocity, e.g., m/sec

The *Gain* in the system (see Figure 7) is $K_x/K_{\dot{x}}$.

The hover cue design is controlled by the selected bandwidth, ω_0 , and the *Gain*, $K_x/K_{\dot{x}}$.

For a given bandwidth, ω_0 , the *Gain* controls the closed-loop dynamics of this system - effectively the speed and damping of the position loop closure response.

As an example, with $\omega_0 = 0.5$ rad/sec, root locus calculations are used to identify a good initial gain selection. As shown in Figure 8, using this example, a loop gain, $K_x/K_{\dot{x}}$ of 0.065 is shown to provide a damping ratio of 0.85 for the two complex poles.

The step response of the ideal hover cue is shown in Figure 9 for this design as well as with variations in bandwidth, ω_0 , while also adjusting the *Gain* to hold the damping ratio objective of 0.85.

The selection of the ω_0 , and the *Gain*, $K_x/K_{\dot{x}}$ is, ultimately, task and vehicle dependent.

The selected hover cue *Gain*, $K_x/K_{\dot{x}}$, and bandwidth, determined by root-locus or other design means using the ideal case (Figure 7), is the initial step in the hover cue design process. From this initial selection, the *Gain* and ω_0 are experimentally refined using test pilot evaluations to tailor the hover cue response as the ideal case is never realizable. Adjustments are necessary to accommodate task (e.g., the task may require fast or slower responses) and vehicle dependencies (e.g., the ideal design may not be realizable due to vehicle nonlinearities or require unacceptably large or rapid attitude changes) for the final hover cue design.

Figure 8: Root Locus for Ideal Hover Cue Loop Closure

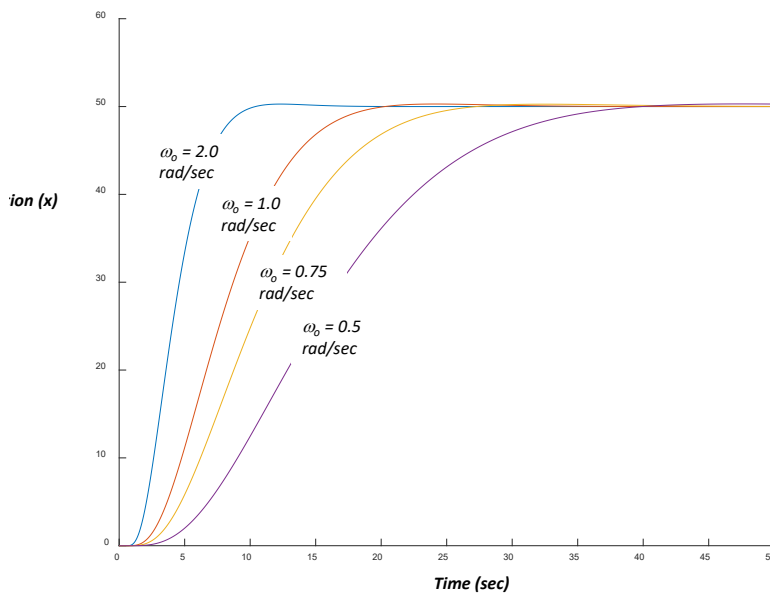


Figure 9: Comparison of ω_0 Variations

3.4. Design

The display scaling, K_{x_s} , is fixed by the display design and navigation range. The value of $K_{\dot{x}}$ is computed from K_x and *Gain* as:

$$K_{\dot{x}} = K_x / Gain$$

The geometry of the integrated symbology set is shown in Figure 10. The figure shows a “range scale” of 500 meters which maps to a physical position on the display (in DUs, e.g., pixels). The conformal landing target (“doghouse” shown in Figure 10) is x_e meters from ownship so it is placed on the display ($x_e * K_x$) DUs in front of ownship. The hover cue (A_x) is computed in DUs (positive forward from ownship).

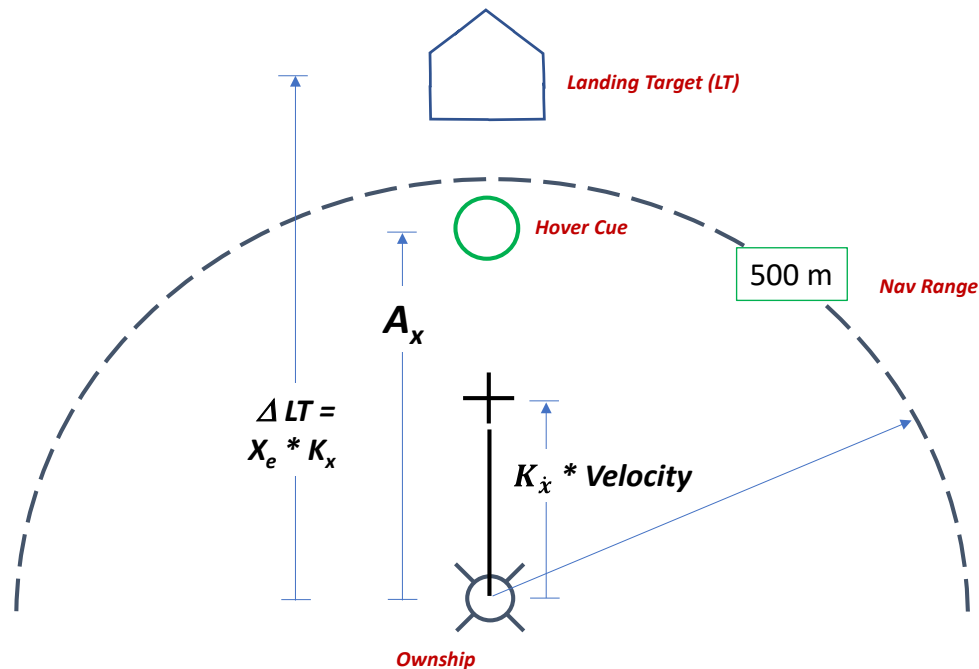


Figure 10: Geometry of Hover Cue Drawing in Display Units (DUs)

3.5. Velocity Vector Portrayal

In addition to controlling the dynamics of the hover cue, the gain selection, $K_x / K_{\dot{x}}$, also determines the physical representation or scaling of the velocity vector on the display (i.e., the length of the velocity vector line).

The *Gain*, $K_x / K_{\dot{x}}$ is in units of sec^{-1} . The length of the velocity vector is scaled by $K_{\dot{x}}$.

Thus, the length of the velocity vector is scaled by $K_{\dot{x}} = K_x / Gain$

As such, the velocity vector length corresponds to $(1 / Gain)$ seconds of distance at the current velocity based on the range scale selection (K_x).

For a *Gain* of 0.065, the length of the velocity vector symbol depicts the distance traveled in 15.4 seconds at the current velocity on the display.

4. Derivation of Hover Cue Control Laws

In the following, the control law mechanization for the hover cue is derived. Caution is advised as this derivation is an example with assumptions of coordinate frame associations that may or may not necessarily hold true.

Also, the derivations are made only for the pitch axis for brevity.

The hover cue longitudinal position is again (*Eqn (1)*):

$$A_x = \frac{\dot{x}K_{\dot{x}}(s + \omega_0)^3}{\omega_0^3}$$

The hover cue control law is derived by first expanding the trinomial of *Eqn (1)*:

$$(s + \omega_0)^3 = s^3 + 3\omega_0s^2 + 3\omega_0^2s + \omega_0^3$$

$$(s + \omega_0)^3 = s(s^2 + 3\omega_0s) + 3\omega_0^2s + \omega_0^3$$

which becomes

$$A_x = \frac{\dot{x}K_{\dot{x}}(s(s^2 + 3\omega_0s) + 3\omega_0^2s + \omega_0^3)}{\omega_0^3}$$

Breaking out equation by multiplication:

$$A_x = \frac{K_{\dot{x}}\dot{x}}{\omega_0^3}s(s^2 + 3\omega_0s) + \frac{K_{\dot{x}}\dot{x}}{\omega_0^3}3\omega_0^2s + \frac{K_{\dot{x}}\dot{x}}{\omega_0^3}\omega_0^3$$

Rearrange and clean-up, the hover cue is:

$$A_x = K_{\dot{x}}\dot{x} + \frac{K_{\dot{x}}\dot{x}}{\omega_0^3}s(s^2 + 3\omega_0s) + 3\frac{K_{\dot{x}}\dot{x}}{\omega_0} \quad \text{Eqn (2)}$$

For translation by rotation, assuming small angles and using pitch as an example as a function of Thrust (T) over mass (m):

$$\begin{aligned} \ddot{x} &= \sin(\theta) \frac{-T}{m} \\ \ddot{x} &= \frac{-T}{m} \theta \end{aligned}$$

The hover cue control law is:

$$A_x = K_{\dot{x}}\dot{x} + \frac{K_{\dot{x}}\dot{x}}{\omega_0^3} \left(\frac{-T}{m} \right) \theta (s^2 + 3\omega_0s) + 3 \frac{K_{\dot{x}}\dot{x}}{\omega_0} \left(\frac{-T}{m} \right) \theta \quad \text{Eqn (3)}$$

4.1. Adaptation for Rate Command, Attitude Hold (RCAH)

The hover cue control law for use with an RCAH flight control system is derived starting with the expansion of *Eqn (3)*:

$$A_x = K_{\dot{x}}\dot{x} + \frac{K_{\ddot{x}}}{\omega_0^3} \left(\frac{-T}{m} \right) (\ddot{\theta} + 3\omega_0\dot{\theta}) + 3 \frac{K_{\dot{x}}}{\omega_0} \left(\frac{-T}{m} \right) \dot{\theta}$$

For the RCAH control law, the following approximation is used:

$$\frac{\dot{\theta}}{\delta} = \frac{K_{RCAH}}{(\tau_{RCAH} s + 1)}$$

The hover cue derivation assumes this transfer function form as an “equivalent aero-system” to the actual spacecraft vehicle response. Other transfer function forms may be more appropriate and the hover cue formulation would need to be adjusted accordingly.

This first-order lag response is a gross approximation to the “ramped” non-aerodynamic pitch attitude rate response of spacecraft as discussed in Section 5.1, but has been shown to provide excellent results since the equivalent aero-system inherently provides response hover cue response filtering. The determination of the gain, K_{RCAH} , and time constant, τ_{RCAH} , is discussed in Section 5.7.

For the RCAH control law:

$$\ddot{\theta} = \frac{K_{RCAH}}{\tau_{RCAH}} \delta - \frac{\dot{\theta}}{\tau_{RCAH}}$$

Substitute and expand:

$$A_x = K_{\dot{x}}\dot{x} + \frac{K_{\ddot{x}}}{\omega_0^3} \left(\frac{-T}{m} \right) \left(\frac{K_{RCAH}}{\tau_{RCAH}} \delta - \frac{\dot{\theta}}{\tau_{RCAH}} \right) + 3 \frac{K_{\dot{x}}}{\omega_0^2} \left(\frac{-T}{m} \right) \dot{\theta} + 3 \frac{K_{\dot{x}}}{\omega_0} \left(\frac{-T}{m} \right) \dot{\theta}$$

The hover cue for a RCAH control law then becomes:

$$A_x = K_{\dot{x}}\dot{x} + \frac{K_{\ddot{x}}}{\omega_0^3} \left(\frac{-T}{m} \right) \left(\frac{K_{RCAH}}{\tau_{RCAH}} \right) \delta + K_{\dot{x}} \left(\frac{-T}{m} \right) \left(\frac{3}{\omega_0^2} - \frac{1}{\omega_0^3 \tau_{RCAH}} \right) \dot{\theta} + 3 \frac{K_{\dot{x}}}{\omega_0} \left(\frac{-T}{m} \right) \dot{\theta}$$

Eqn (4)

4.2. Results – Hover Cue Compared to Explicit Guidance

An experiment was conducted evaluating explicit pitch/roll guidance against the hover cue during lunar landing. The piloting task included landing site redesignations (i.e., lateral offsets) using 15, 30, and 45 deg “glideslopes” – approaching more operationally realistic trajectories under the Constellation Program. Details are contained in Reference 17.

The data generally showed that explicit guidance was good: it provided simple and straight-forward command information to meet the task demands. The display was unambiguous and clear.

Unfortunately, the command guidance required precision on the part of the evaluation pilots to track the attitude to achieve desired performance. The vehicle could significantly

overshoot or undershoot the guidance, generating low altitude corrections and increased workload on the part of the pilot to use the guidance to land on the landing target.

In general, the data showed a one to two rating improvement (using the Cooper-Harper scale) on average indicating better task performance and/or lower pilot workload when using the hover cue. In particular, for low control power configurations, the pilots were able to achieve even better task performance compared to explicit pitch/roll command guidance by being able to develop compensation techniques when using the hover cue. The pilots were not “blindly” following explicit pitch/roll guidance but instead, had a visual depiction of the distance to the landing target, the effect of their inputs on the velocity and acceleration of the vehicle, and a visual depiction of the instantaneously computed hover point. The pilots were able to use this information to their advantage to construct control strategies that yielded improved performance and workload, without exciting overcontrol and pilot-induced oscillation tendencies.

The hover cue also showed promise when used in a head-worn display application for lunar landing but additional work was recommended in terms of tailoring the hover cue concept for a small field-of-view, conformal display (see Ref. 18).

4.3. Adaptation for Attitude-Command, Velocity Hold (ACVH):

In conjunction with the Autonomous Landing and Hazard Avoidance Technology project, simulator evaluations were conducted (Ref. 19) evaluating control law enhancements to improve the handling qualities challenges of returning to the moon.

One control law concept showing promise for precise hover positioning, especially with configurations that do not have control power that meets Cheatham-Hackler, was an Attitude Command, Velocity Hold (ACVH) control law. The rotational hand controller commands a vehicle attitude proportional to the inceptor input; when the input is removed, the control law holds the current velocity. The ACVH is a control law type representative of helicopter control modes.

A key feature of the ACVH, as applied to spacecraft, is the Hover-Hold, Incremental Position Control (HH/IPC) mode. When the translational velocity is slow enough and the pilot relaxes or releases the control inceptor, the control law drops out of ACVH and into the HH/IPC mode. The HH/IPC mode automatically maintains its longitudinal position (hover hold) and the pilot can change that position incrementally using the IPC mode.

For the spacecraft final approach and landing task, learning the proper flying technique has been found to be challenging for some pilots. The hover cue was adapted to the ACVH control law, as follows, to assist the pilots.

The derivation of the hover cue control law for an ACVH flight control design is given in Appendix A.

The derivation starts with the general hover cue equation, *Eqn (3)*, and is rearranged to be:

$$A_{\dot{x}} = K_{\dot{x}}\dot{x} + 3\frac{K_{\dot{x}}}{\omega_o}\left(\frac{-T}{m}\right)\theta + \frac{K_{\dot{x}}}{\omega_o^3}\left(\frac{-T}{m}\right)\ddot{\theta} + \frac{K_{\dot{x}}}{\omega_o^3}\left(\frac{-T}{m}\right)3\omega_o\dot{\theta}$$

For the ACVH control law, the pitch attitude response from stick input is assumed to be:

$$\left(\frac{\theta}{\delta}\right) = \left(\frac{K_{ACVH}\omega_{ACVH}^2}{s^2 + 2\zeta\omega_{ACVH}s + \omega_{ACVH}^2}\right)$$

where K_{ACVH} , ζ_{ACVH} , and ω_{ACVH} describe the transfer function response characteristics of the closed-loop vehicle.

Note again, the hover cue derivation assumes this transfer function form as an “equivalent aero-system” to the actual spacecraft vehicle response. Other transfer function forms may be more appropriate and the hover cue formulation would need to be adjusted accordingly. This second-order transfer function response is a gross approximation to the non-aerodynamic pitch attitude response of spacecraft but has been shown to provide excellent results as it provides hover cue response filtering, see Section 5.1.

The hover cue control law for the ACVH flight control system is derived (shown in Appendix A) by substituting the assumed closed-loop ACVH into the hover cue equation:

$$\begin{aligned} A_{\dot{x}} = & K_{\dot{x}}\dot{x} + K_x \left(\frac{-T}{m}\right) \left[\frac{3}{\omega_o} - \frac{\omega_{ACVH}^2}{\omega_o^3}\right] \theta \\ & + K_{\dot{x}} \left(\frac{-T}{m}\right) \left[\frac{K_{ACVH}\omega_{ACVH}^2}{\omega_o^3}\right] \delta + K_{\dot{x}} \left(\frac{-T}{m}\right) \left[\frac{3}{\omega_o^2} - \frac{2\zeta\omega_{ACVH}}{\omega_o^3}\right] \dot{\theta} \end{aligned}$$

4.4. Hover Cue with ACVH and RCAH

The hover cue accurately portrays the continuously-computed hover point for both the RCAH and ACVH control laws but the pilot control actions are very different, reflective of the different control laws. So while the hover cue “works,” the handling characteristics are very different.

An experiment was conducted comparing the ACVH versus RCAH flight control systems in the lunar landing final approach and landing task (Ref. 20).

One adaptation to the RCAH control law was made for the experiment for comparative purposes with the ACVH control law: a pilot-commanded HH/IPC mode was added to the RCAH control law.

This mode was added to relieve the pilot of position control during the vertical descent to landing to enable a one-to-one comparison of the two control system designs.

For RCAH, the vehicle position is normally held using the hover cue during the vertical descent phase, but pilot comments indicated that it creates pilot workload. (The pilots ended up trying to maintain <1 m precision in the landing at a cost of pilot workload and attention to the hover cue.)

The advantage of the HH/IPC mode is that it allowed the pilots the freedom to scan OTW and head-down with the LIDAR (Light Detection and Ranging) and/or camera views to confirm the landing site was free of hazards, without having to attend to their longitudinal

position. The pilot could also yaw (rotate) the vehicle to a heading optimal for power or communication concerns during the vertical descent phase without coupling into the pitch/roll rotational hand controller interceptor.

The experimental data showed that better handling qualities were attained with the RCAH control laws in comparison to the ACVH control laws.

The hover cue for both control laws was shown to significantly improve the pilot's ability to control translation and create satisfactory handling qualities especially for otherwise, sluggish configurations that don't meet the Cheatham-Hackler criterion. In both cases, the hover cue was a valuable manual control display augmentation.

The pilots demonstrated better performance and lower frustration levels with RCAH as compared to ACVH during the manual redesignation landing task. The reasons for this improvement were not associated with the hover cue or its design, but were tied to the control law attributes (see Ref. 20 for details).

These results, at least for the control powers tested, imply simple RCAH control laws can be used – saving software development and pilot training costs – at the modest expense of a display augmentation.

HH/IPC, as a sub-mode of RCAH control law, was recommended.

5. Practical Application Experience

In the course of hover cue development and spacecraft handling qualities evaluations with and without the hover cue, some lessons were learned that have helped in the practical applications of the hover cue.

5.1. Non-atmospheric flight considerations

RCS jet firings are typically on-off firings that can cause jerky movements of the hover cue. Smoothing (i.e., filtering) has been applied to the pilot control input signals to temper (somewhat) the jerkiness of the symbol movement due to the discrete nature of the RCS firings.

Also, the approximations of a first-order time constant response (τ_{RCAH}) for a spacecraft RCAH design and a second-order frequency (ω_{ACVH}) and damping ratio (ζ_{ACVH}) response for an ACVH design are intentional. By using these transfer function approximations, additional smoothing of the hover cue is provided.

5.2. Bandwidth Selection

Experimentation has indicated that a hover cue bandwidth selection ($\omega\theta$) between 0.5 and 1.0 rad/sec is a reasonable value for the spacecraft RCAH control law considering the piloting demands for this task and the relatively sluggish nature of vehicle dynamics being considered as “representative” for a lunar landing mission.

Other bandwidths can be used, as necessary and appropriate, with *Gain* changes also being needed simultaneously to keep the loop closure stable. For example, see Figure 9.

The bandwidth selection is vehicle and task dependent.

5.3. ND Range / Range Control

The *Gain* selection, K_x/K_x is held constant, but the display range scale (e.g., the range selection on the ND) should be sized and may be varied to enable precision landing.

The ND range selection, K_x , is typically adjusted automatically using discrete step sizes to keep the landing target conformally on the screen with sufficient fidelity for precision control. The ND range selection is typically driven by a look-up table based upon the range to the conformal landing target, with hysteresis to avoid potential chatter. This selection is task and display dependent, balancing precision of control against an excessive number of range scale variations.

Other ranging concepts, such as nonlinear ranging or continuous ranging, have been explored and may be practical depending upon the application.

When using the hover cue on camera overlays, the display range scale is estimated using height above the terrain.

5.4. Instantaneous Center-of-Rotation Compensation

The hover cue was developed initially for spacecraft controlled by Reaction Control System (RCS) jets whose design effectively creates rotation about the center-of-mass (cm) without significantly imparting translational acceleration.

For vehicles that use engine gimbaling, this assumption is invalid. Engine gimbaling typically creates a non-minimum phase-type response as the horizontal thrust component in the initial response is opposed to the desired direction of flight, as illustrated in Figure 11, where

- T is Thrust
- cm is the center-of-mass (m)
- l is the distance from the cm to the thrust application point
- x is the forward direction of flight
- θ is the vehicle pitch attitude (in aircraft coordinate frame)
- δ_q is the pitch gimbal angle of the engine
- ICR is the Instantaneous Center-of-Rotation
- l_{pitch} is the vertical distance from the cm to ICR

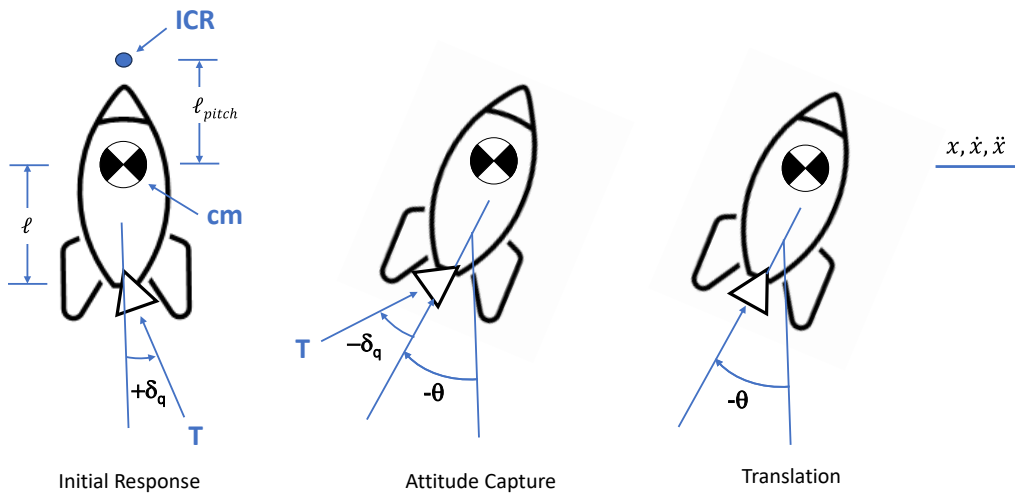


Figure 11: Translation by Rotation using Engine Gimballing

This non-minimum phase response induces undesirable hover cue movement using the hover cue of Eqn 2.

The derivation of hover cue control law with engine gimbaling for control is given in Appendix B.

The derivation starts with the translational acceleration at cm under engine gimbaling being:

$$\ddot{x} = \frac{-T}{m} \sin(\delta_q + \theta)$$

The Instantaneous Center-of-Rotation (ICR) position, l_{pitch} (i.e., ICR position relative to cm , positive down), is:

$$l_{pitch} = \frac{I_{yy}}{-\ell \cdot m}$$

where:

m is the vehicle mass

ℓ is the distance from the cm to the thrust application point

I_{yy} is the pitch inertia (in an aircraft body coordinate frame)

Velocity (\dot{x}) and acceleration (\ddot{x}) at the ICR (assuming zero lateral offset of the gimbal from the cm in the “aircraft” body X,Y axes) follows from the general equations:

$$\dot{x}_{ICR} = \dot{x}_{CM} + (\vec{\omega} \times \vec{r})$$

and

$$\ddot{x}_{ICR} = \ddot{x}_{CM} + (\vec{\omega} \times (\vec{\omega} \times \vec{r})) + (\dot{\vec{\omega}} \times \vec{r})$$

yielding, for pitch/longitudinal only:

$$\dot{x}_{ICR} = \dot{x}_{cm} + q \cdot l_{pitch}$$

$$\ddot{x}_{ICR} = \ddot{x}_{cm} + \dot{q} \cdot l_{pitch} - p \cdot r \cdot l_{pitch}$$

It is assumed that the contribution of cross-coupling terms in acceleration will be negligible, that is:

$$\ddot{x}_{ICR} = \ddot{x}_{cm} + \dot{q} \cdot l_{pitch}$$

For gimbaling control, the acceleration at the ICR becomes:

$$\ddot{x}_{ICR} = \frac{-T}{m} \sin(\delta_q + \theta) + \dot{q} \frac{I_{yy}}{-\ell \cdot m}$$

The hover cue control law for engine gimbaling is derived (see Appendix B) using from Eqn (2) (repeated here):

$$A_x = K_{\dot{x}} \dot{x} + \frac{K_x \ddot{x}}{\omega_0^3} s(s^2 + 3\omega_0 s) + 3 \frac{K_x \ddot{x}}{\omega_0} \quad Eqn (2)$$

by substituting \ddot{x}_{ICR} in place of $\ddot{x}_{CM}(\ddot{x})$ and \dot{x}_{ICR} in place of $\dot{x}_{CM}(\dot{x})$ and assuming that $\sin(\delta_q + \theta) = \sin(\delta_q) + \sin(\theta)$:

$$A_x = K_{\dot{x}} \dot{x}_{ICR} + \left(-\frac{K_x}{\omega_0^3} \left(\frac{-T}{m} \right) \left(\frac{T\ell}{I_{yy}} \right) \right) \sin(\delta_q) + \frac{K_x}{\omega_0^3} \left(\frac{-T}{m} 3\omega_0 \right) \dot{\theta} + 3 \frac{K_x}{\omega_0} \left(\frac{-T}{m} \sin(\theta) \right) \quad Eqn(5)$$

For RCAH control law, we, again, use the “equivalent aero-system” approximation that:

$$\frac{\dot{\theta}}{\delta} = \frac{K_{RCAH}}{(\tau_{RCAH} s + 1)}$$

The hover cue control law for a RCAH flight control system that employs engine gimbaling as the control effector, using cm reference, is:

$$A_x = K_{\dot{x}}(\dot{x}_{cm} + q \cdot l_{pitch}) + \frac{K_{\dot{x}}}{\omega_0^3} \left(\frac{-T}{m} 3\omega_0 \right) (K_{RCAH} \delta) + \frac{K_{\dot{x}}}{\omega_0^3} \left(\frac{-T}{m} \right) \left(\frac{T\ell}{I_{yy}} \right) (3\omega_0(\tau_{RCAH}) - 1) \sin(\delta_q) + 3 \frac{K_{\dot{x}}}{\omega_0} \left(\frac{-T}{m} \right) \sin(\theta) \quad Eqn (6)$$

The hover cue differences (for the RCAH control law) with RCS versus gimballed engine control effectors are shown by comparing *Eqn (4)* and *Eqn (6)*. The primary differences are: 1) the translational velocity for the engine gimballed controller includes the ICR effect; and, 2) the pitch rate term in the RCS controller hover cue is replaced by an engine gimballed control term. (Also, *Eqn (4)* assumes a small angle approximation for pitch angle, θ ; see Section 6.2).

5.5. RCAH and ACVH Characteristic Values

The hover cue dynamics are varied based upon the values of K_{RCAH} and τ_{RCAH} for an RCAH flight control system and by K_{ACVH} , ζ_{ACVH} , and ω_{ACVH} for an ACVH flight control system design.

These values need to be approximated for non-atmospheric vehicles that use RCS or Engine Gimbaling / Thrust Vectoring Control (TVC) as their primary attitude control effectors.

5.5.1. RCAH K Values

With the assumed RCAH transfer function form:

$$\frac{\dot{\theta}}{\delta} = \frac{K_{RCAH}}{(\tau_{RCAH} s + 1)}$$

the value of K_{RCAH} equals the maximum steady-state attitude rate response.

5.5.2. RCAH τ Values

As discussed in Section 5.1, the approximation of using a first-order time constant for a spacecraft RCAH design is intentional. By using the first-order filter approximation, smoothing of the hover cue is provided and a precise value has not been found to be critical.

The τ_{RCAH} value should be determined from the rotational control power (CP) as follows.

The CP (deg/sec²) is computed for RCS control by the RCS jet size times their moment arm, divided by the inertia:

$$CP = T_{RCS} l_{RCS} / I_{yy}$$

where:

T_{RCS} is the RCS total jet thrust

l_{RCS} is the effective moment arm

I_{yy} is the inertia

This computation of control power ignores possible jet-switching logic that may or may not be important to the design and if important, would need to be considered in the hover cue implementation.

For engine gimbaling configurations, the CP is less easily defined. For consistency, the following has been applied:

- CP is computed using the “nominal” thrust value (T) during the approach and landing phase:

$$CP = - \left(\frac{T \ell}{I_{yy}} \right) \sin(\delta_{q_limit})$$

where δ_{q_limit} is the maximum gimbal deflection.

Then, for both engine gimbaling and RCS control effectors, the τ_{RCAH} for RCAH hover cue is computed as:

$$\tau_{RCAH} = (\text{Rate}_{ss_1/3} / CP) * 0.632$$

where:

- $\text{Rate}_{ss_1/3}$ is the steady-state attitude rate for a one-third stick input
- $(\text{Rate}_{ss_1/3} / CP)$ will be the time to reach the commanded, attitude rate ($\text{Rate}_{ss_1/3}$) with a stick step input.
- 0.632 will be the time to the equivalent 1st order time constant value.

An example RCS-commanded, RCAH control law response (labeled “RCS-RCAH Response”) to a one-third stick input (i.e., ignoring phase-plane logic, deadbanding, etc.) is shown in Figure 12 for an RCAH design using control power (CP) of 2.13 deg/sec² and a maximum steady-state rate command of 12 deg/sec. The $\text{Rate}_{ss_1/3}$ is 4.0 deg/sec. The time-to-reach the 63% of the steady-state rate is 1.2 sec. The hover cue RCAH response (labeled “Hover Cue RCAH Assumed Response”) for the one-third stick input follows the RCS RCAH control law response initially and provides a longer tail in reaching the steady-state value. Experience has shown that this tail is desirable for filtering.

By using this method to compute the τ_{RCAH} value, inaccuracies in tracking the spacecraft RCAH response are intentional. The time constant value calculations shown above are not nor do they need to be exact for good hover cue handling qualities.

As another example, when using the same hover cue value of τ_{RCAH} for larger stick inputs (as shown in Figure 13 for a two-thirds stick input), the hover cue response (labeled

“Hover Cue RCAH Assumed Response”) will lead the actual rate response labeled “RCS-RCAH Response”). For stick inputs larger than assumed one-third stick command for the τ_{RCAH} calculation, the hover cue is more responsive than the vehicle response which is designed to *help*, in theory, reduce a propensity for the pilot to use larger, possibly inappropriate inputs.

The choice of a one-third stick command for the τ_{RCAH} calculation was determined by experience.

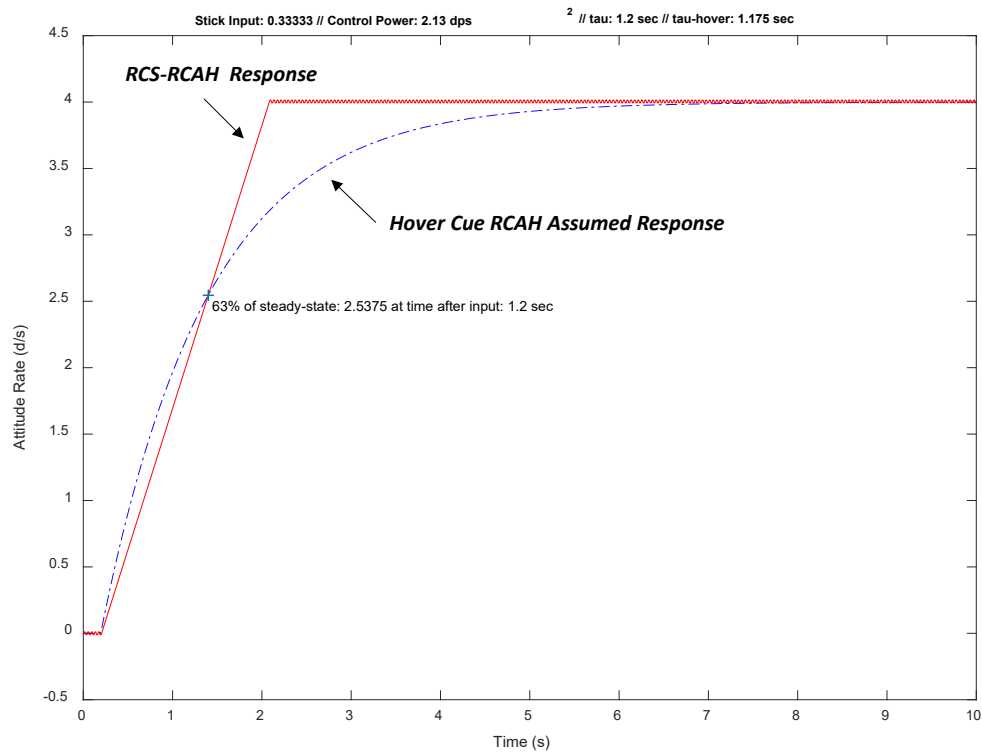


Figure 12: Example RCAH-RCS Time Response for One-Third Stick Input

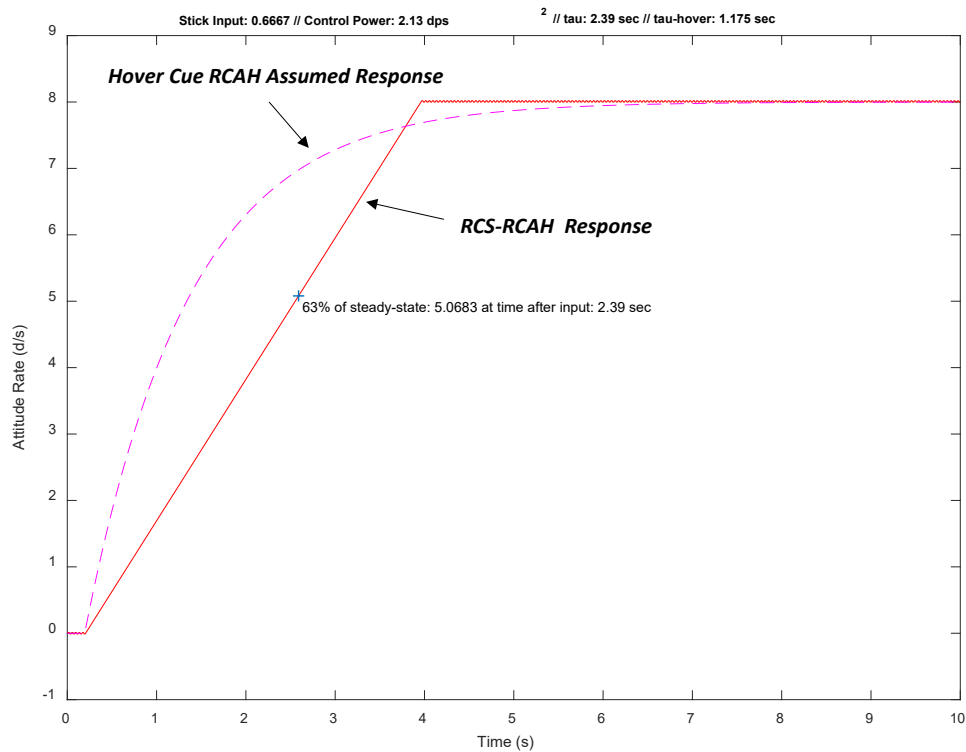


Figure 13: Example RCAH-RCS Time Response for Two-Thirds Stick Input

5.5.3. ACVH K Values

With the assumed form of the ACVH equivalent transfer function:

$$\left(\frac{\theta}{\delta}\right) = \left(\frac{K_{ACVH}\omega_{ACVH}^2}{s^2 + 2\zeta\omega_{ACVH}s + \omega_{ACVH}^2}\right)$$

the value of K_{ACVH} is set by the ACVH control law design for the maximum attitude achieved with full rotational hand controller input.

5.5.4. ACVH ω and ζ Values

The hover cue damping (ζ) and the frequency (ω) values for the ACVH hover cue are based upon the ACVH control law design and the resultant equivalent aero-system response. A general procedure to determine these values has not been developed.

For an RCS-effected ACVH control law for the HLS GRM vehicle, the current hover cue design uses:

$$\zeta_{ACVH} = 1.0$$

$$\omega_{ACVH} = 1.5 \text{ rad/sec}$$

The damping ratio (ζ_{ACVH}) and frequency (ω_{ACVH}) values are not nor do they need to be exact for good hover cue handling qualities. The selected values only need to approximate the dynamic response of the augmented vehicle dynamics.

6. Improvements

The hover cue showed significant promise during spacecraft handling qualities experimentation. It was, however, not without deficiencies warranting improvement.

It should be noted that the hover cue implementation described above is a “pure” implementation. As a demonstration tool, this “pure” implementation is perfectly suitable to showcase what it is and how it works. However, the “pure” hover cue is not perfect and the pilots often see these impurities.

Of significant note is that the implementation assumes the linear transfer function characteristics are valid.

The following improvements are being evaluated to address pilot comments to make the hover cue:

- More flyable
- More intuitive
- Less prone to overcontrol

6.1. Hover Cue vs. Modified Acceleration Ball

Pilots sometimes don’t understand what the hover cue is “telling them” especially when they are *not* making control inputs.

Using the RCAH hover cue as an example, the hover cue control law is repeated here:

$$A_x = K_{\dot{x}}\dot{x} + \frac{K_{\dot{x}}}{\omega_0^3} \left(\frac{-T}{m} \right) \left(\frac{K_{RCAH}}{\tau_{RCAH}} \right) \delta + K_{\dot{x}} \left(\frac{-T}{m} \right) \left(\frac{3}{\omega_0^2} - \frac{1}{\omega_0^3 \tau_{RCAH}} \right) \dot{\theta} + 3 \frac{K_{\dot{x}}}{\omega_0} \left(\frac{-T}{m} \right) \theta$$

When there are no pilot inputs (δ), the hover cue is essentially a modified acceleration cue:

$$A_x = K_{\dot{x}}\dot{x} + K_{\dot{x}} \left(\frac{-T}{m} \right) \left(\frac{3}{\omega_0^2} - \frac{1}{\omega_0^3 \tau_{RCAH}} \right) \dot{\theta} + 3 \frac{K_{\dot{x}}}{\omega_0} \left(\frac{-T}{m} \right) \theta$$

The hover cue shows the acceleration status of the vehicle. It does *not* indicate the continuously-computed hover position, unless, of course, $\dot{x} = \dot{\theta} = \theta = 0$.

The improvement is in the form of pilot awareness. The pilot is informed of this transition by changing the color of the hover cue:

- The hover cue is colored Green only when the $abs(\delta) > Value$;
- Otherwise (i.e., the $abs(\delta) < Value$), the hover cue is colored White.

The *Value* term should correspond to the deadband or breakout displacement of the inceptor.

With this change:

- The color indicates to the pilot when the symbol is a hover cue (i.e., Green)
- And, when the symbol is a modified acceleration cue (i.e., White).

This implementation can be used in all instantiations of the hover cue (i.e., for RCAH and ACVH control laws and with gimballed engines for control).

Piloted demonstrations have shown that this is a desirable change.

6.2. Large attitude operations

The pilot sometimes drops attitude out of their cross-check when flying the hover cue. The hover cue is often used as their primary control element; it is located on the ND and attitude is not a salient feature on this display, if shown at all.

It is possible that the pilot becomes unaware when using the hover cue and this can be misleading as pitch/roll attitudes become large.

The hover cue is a linear interpretation and if the vehicle is in a non-linear regime, such as gimbal-limited operations, the hover cue can be misleading.

6.2.1. Remove Small Angle Approximations

To remove this ambiguity, the small angle approximations in the hover cue are removed.

The hover cue computations are changed such that the θ function in the RCAH and ACVH pitch hover cues use $\sin(\theta)$.

For RCAH pitch example:

$$A_x = K_{\dot{x}}\dot{x} + \frac{K_{\dot{x}}}{\omega_0^3} \left(\frac{-T}{m} \right) \left(\frac{K_{RCAH}}{\tau_{RCAH}} \right) \delta + K_{\dot{x}} \left(\frac{-T}{m} \right) \left(\frac{3}{\omega_0^2} - \frac{1}{\omega_0^3 \tau_{RCAH}} \right) \dot{\theta} + 3 \frac{K_{\dot{x}}}{\omega_0} \left(\frac{-T}{m} \right) \theta$$

$$A_x = K_{\dot{x}}\dot{x} + \frac{K_{\dot{x}}}{\omega_0^3} \left(\frac{-T}{m} \right) \left(\frac{K_{RCAH}}{\tau_{RCAH}} \right) \delta + K_{\dot{x}} \left(\frac{-T}{m} \right) \left(\frac{3}{\omega_0^2} - \frac{1}{\omega_0^3 \tau_{RCAH}} \right) \dot{\theta} + 3 \frac{K_{\dot{x}}}{\omega_0} \left(\frac{-T}{m} \right) \mathbf{\sin}(\theta)$$

6.2.2. Limiters

One way to limit the propensity of a pilot to enter into nonlinear flight characteristics while using the hover cue is to not display the hover cue until the velocity and/or distance to the landing zone is less than some appropriate value. Without the symbol being shown, the pilot is less likely to overcontrol the vehicle using the hover cue. The pilot would have to utilize other symbology/information (attitude and velocity) for vehicle control.

Alternatively, the hover cue formulations may be modified by adding additional terms to restrict the hover cue movement in the form of limiters. For example, using RCAH with RCS control, the RCAH formulation is refined as follows:

$$A_x = K_{\dot{x}}\dot{x} + \frac{K_{\dot{x}}}{\omega_0^3} \left(\frac{-T}{m} \right) \left(\frac{K_{RCAH}}{\tau_{RCAH}} \right) \delta + K_{\dot{x}} \left(\frac{-T}{m} \right) \left(\frac{3}{\omega_0^2} - \frac{1}{\omega_0^3 \tau_{RCAH}} \right) \dot{\theta} + 3 \frac{K_{\dot{x}}}{\omega_0} \left(\frac{-T}{m} \right) \sin(\theta) + K_{\dot{x}} Limit_{vx} + K_{\dot{x}} Limit_{\theta}$$

Where:

$$Limit_{vx} = K_{lim_vx} * \begin{cases} (abs(\dot{x}) - Vx_{lim}) * sign(\dot{x}) & \text{when } (abs(\dot{x}) - Vx_{lim}) > 0 \\ 0. & (abs(\dot{x}) - Vx_{lim}) < 0 \end{cases}$$

$$Limit_{tht} = K_{lim_tht} * \begin{cases} (abs(\theta) - THT_{lim}) * sign(\theta) & \text{when } (abs(\theta) - THT_{lim}) > 0 \\ 0. & (abs(\theta) - THT_{lim}) < 0 \end{cases}$$

The limiter values are computed based on the characteristics of the vehicle and the task.

For example, the HLS Government Reference Model (HLS GRM) (Ref. 21) limiters are set at:

- 20 deg for pitch (THT_{lim})
- 20 m/sec for the forward velocity limiter (VX_{lim}).

Additional features to note:

- The hover cue should change color to indicate that a limiter is in effect for pilot awareness (e.g., the hover cue should change to amber with either attitude or velocity limiters are in effect for immediate pilot awareness and subsequent action.) This change unto itself is a powerful cue alerting the pilot that the attitude and/or velocity is reaching large values.
- The gain values K_{lim_vx} and K_{lim_tht} are 0.02 and -0.5, respectively, for the HLS GRM. These values would need to be adjusted depending upon the specific vehicle implementation.
- The limiters, shown above, are linear beyond the limit values, ramping up proportionally. Other designs may be more appropriate depending upon the vehicle design. For instance, a parabolic shaping after the limit value is currently being used with the HLS GRM to more smoothly introduce the limiters.

6.3. Improvement Summary

The addition of limiters, alerting, and other control law tailoring should be considered in a final hover cue implementation.

The hover cue has been shown to improve the handling qualities of otherwise deficient characteristics.

However, it is also possible that Pilot-Induced Oscillation (PIO) conditions can be triggered by a pilot who might use inappropriately large or aggressive control inputs if blindly following the hover cue. While the hover cue may ameliorate PIO tendencies to some degree, it is not a panacea. The propensity for PIO is quite often tied to the inherent sluggish control responsiveness or response latency of the vehicle.

7. Concluding Remarks

A display/control element - a hover cue - has been developed for specific application to a spacecraft's final approach and landing task on the Moon or other airless body. This hover cue is a symbol that can be placed on the pilot's head-down Navigation Display or on a head-up display in a conformal view that provides feedback to the pilot on the control inputs required to translate to the hover cue location.

The key advantage to the hover cue over other methods such as explicit pitch/roll command guidance is that it is not tied to the vehicle's flight guidance system. The pilot can quickly and easily translate the vehicle to a new location without reliance on or interaction with the flight guidance system. Human-in-the-loop testing shows that flying a configuration with a hover cue yields a 1 to 2 rating improvement on average (in terms of Cooper-Harper pilot ratings) compared to flying the same configuration using pitch/roll command guidance (Ref. 17).

This report provides the background in the development of the hover cue, guidance for the hover cue design, and some notable changes based on experimentation. Experimental testing is referenced for those desiring additional information.

Augmentation of the hover cue to address some of its limitations are also discussed. These augmentations are desirable for real-world implementations.

References

- 1) Cheatham, D.C., and Hackler, C.T., "Handling Qualities for Pilot Control of Apollo Lunar-Landing Spacecraft," *Journal of Spacecraft*, Vol. 3, No. 5, May 1966.
- 2) Matranga, G.J. and Walker, J.A., "An Investigation of Terminal Lunar Landing with the Lunar Landing Research Vehicle," NASA-TM-X-74475. 1965.
- 3) Hackler, C.T., Brickel, J.R., Smith, H.E., and Cheatham, D.C., "Lunar Module Pilot Control Considerations," NASA TN D-4131, February 1968
- 4) Cheatham, D.C., and Bennett, F.V., "Apollo Lunar Module Landing Strategy," in *Apollo Lunar Landing Symposium* (pp. 175-240), June 1966.
- 5) Major, L.M, Brady, T.M., and Paschall II, S.C., "Apollo Looking Forward: Crew Task Challenges," paper presented at the 2009 IEEE Aerospace Conference, 7-14 March 2009.
- 6) Bellman, D.R. and Matranga, G.J., "Design and Operational Characteristics of a Lunar-Landing Research Vehicle," NASA-TN-D-3023, 1965.
- 7) Fincannon, J., "Lunar South Pole illumination: review, reassessment, and power system implications." In *5th International Energy Conversion Engineering Conference and Exhibit (IECEC)*, June 2007.
- 8) Cohanin, B.E., Fill, T.J., Paschall, S., Major, L.M. and Brady, T., "Approach Phase ΔV Considerations for Lunar Landing." In *2009 IEEE Aerospace Conference*, March 2009.
- 9) NASA Broad Agency Announcement of Next Space Technologies for Exploration Partnerships -2, Appendix H: Human Landing System, Attachment F, HLS-RQMT-001. Retrieved 1/6/2025 at <https://sam.gov/opp/d5460a204ab23cc0035c088dcc580d17/view>
- 10) Jarvis, C.R., "Flight-Test Evaluation of an On-Off Rate Command Attitude Control System of a Manned Lunar-Landing Research Vehicle," NASA-TND-3903, 1967.
- 11) Stengel, R.F. (1970): *Manual Attitude Control of the Lunar Module*. *Journal of Spacecraft*, Vol. 7, No. 8, August 1970.
- 12) Bilimoria, K.D., "Effects of Control Power and Guidance Cues on Lunar Lander Handling Qualities," paper presented at the AIAA SPACE 2008 Conference and Exposition, AIAA Paper 2008-7799, San Diego, California, 9-11 September 2008.
- 13) Cooper, G.E., and Harper, Jr., R.P.: *The Use of Pilot Rating in the Evaluation of Aircraft Handling Qualities*. NASA TN D-5153, April 1969.
- 14) Schroeder, J.A. and Merrick, V.K.: "Control and Display Combinations for Blind Vertical Landings." *Journal of Guidance, Control, and Dynamics*, Vol. 15, No. 3, May-June 1992, pp. 751-760.

- 15) Corliss, L. D., and Dugan, D.C. "A VTOL translational rate control system study on a six degrees-of-freedom motion simulator." NASA-TM-X-62194. 1972.
- 16) Neiswander, G.M., "Improving rotorcraft deceleration guidance for brownout landing," Doctoral dissertation, Master's Thesis at The University of Iowa. 2010.
- 17) Bailey, R.E., Jackson, E.B. and Arthur, J.J., "Handling qualities implications for crewed spacecraft operations." In 2012 IEEE Aerospace Conference (pp. 1-20), March 2012.
- 18) Arthur III, J.J., Bailey, R.E, Jackson, E.B., Barnes, J.R., Williams, S.P., and Kramer, L.J., "Part-task simulation of synthetic and enhanced vision concepts for lunar landing." In Enhanced and Synthetic Vision 2010, Vol. 7689, pp. 43-55. SPIE, 2010.
- 19) Duda, K.R., Johnson, M.C., and Fill, T.J., "Design and Analysis of Lunar Lander Manual Control Modes." Paper presented at the 2009 IEEE Aerospace Conference, 7-14 March 2009.
- 20) Kramer, L.J., Bailey, R.E., Neuhaus, J.R., Dugan, T.H., Couch, J.C. and Jackson, E.B., "Handling Qualities Assessment of Manual Lunar Landing with Display Augmentation." In 2023 IEEE Aerospace Conference (pp. 1-14), March 2023.
- 21) Lugo, R.A., Dwyer-Cianciolo, A., Dutta, S., Williams, R.A., Green, J.S., Chen, P., D'Souza, S., and Pensado, A.R. "Precision Landing Performance of a Human-Scale Lunar Lander Using a Generalized Simulation Framework." paper presented at AIAA SciTech 2022 Forum, Jan. 3-7, 2022, San Diego, CA.

Appendix A: ACVH Hover Cue Derivation

The derivation of the hover cue control law for an ACVH flight control design is as follows.

The hover cue control law for an ACVH flight control design starts with the general equation repeated here (Eqn (3)):

$$A_x = K_{\dot{x}}\dot{x} + \frac{K_{\ddot{x}}}{\omega_0^3} \left(\frac{-T}{m} \right) \theta (s^2 + 3\omega_0 s) + 3 \frac{K_{\dot{x}}}{\omega_0} \left(\frac{-T}{m} \right) \dot{\theta}$$

Rearranging the equation:

$$A_{\dot{x}} = K_{\dot{x}}\dot{x} + 3 \frac{K_{\ddot{x}}}{\omega_0} \left(\frac{-T}{m} \right) \theta + \frac{K_{\ddot{x}}}{\omega_0^3} \left(\frac{-T}{m} \right) (s + 3\omega_0) \dot{\theta}$$

$$A_x = K_{\dot{x}}\dot{x} + 3 \frac{K_{\ddot{x}}}{\omega_0} \left(\frac{-T}{m} \right) \theta + \frac{K_{\ddot{x}}}{\omega_0^3} \left(\frac{-T}{m} \right) \ddot{\theta} + \frac{K_{\dot{x}}}{\omega_0^3} \left(\frac{-T}{m} \right) 3\omega_0 \dot{\theta}$$

We apply the assumption that an ACVH control law is described as:

$$\left(\frac{\theta}{\delta} \right) = \left(\frac{K_{ACVH} \omega_{ACVH}^2}{s^2 + 2\zeta \omega_{ACVH} s + \omega_{ACVH}^2} \right)$$

where K_{ACVH} , ζ_{ACVH} , and ω_{ACVH} describe the transfer function response characteristics of the closed-loop vehicle.

Deconstructing yields:

$$\ddot{\theta} = K_{ACVH} \omega_{ACVH}^2 \delta - 2\zeta \omega_{ACVH} \dot{\theta} - \omega_{ACVH}^2 \theta$$

Substituting back:

$$A_x = K_{\dot{x}}\dot{x} + 3 \frac{K_{\ddot{x}}}{\omega_0} \left(\frac{-T}{m} \right) \theta + \frac{K_{\ddot{x}}}{\omega_0^3} \left(\frac{-T}{m} \right) (K_{ACVH} \omega_{ACVH}^2 \delta - 2\zeta \omega_{ACVH} \dot{\theta} - \omega_{ACVH}^2 \theta) + K_{\dot{x}} \left(\frac{-T}{m} \right) \left(\frac{3}{\omega_0^2} \right) \dot{\theta}$$

Expanding and Regrouping:

$$A_x = K_{\dot{x}}\dot{x} + \left[3 \frac{K_{\ddot{x}}}{\omega_0} \left(\frac{-T}{m} \right) + \frac{K_{\ddot{x}}}{\omega_0^3} \left(\frac{-T}{m} \right) (-\omega_{ACVH}^2) \right] \theta + \frac{K_{\dot{x}}}{\omega_0^3} \left(\frac{-T}{m} \right) [K_{ACVH} \omega_{ACVH}^2] \delta + \left[\frac{K_{\dot{x}}}{\omega_0^3} \left(\frac{-T}{m} \right) (-2\zeta \omega_{ACVH}) + K_{\dot{x}} \left(\frac{-T}{m} \right) \left(\frac{3}{\omega_0^2} \right) \right] \dot{\theta}$$

With a little clean-up, the hover cue control law for the ACVH flight control system becomes:

$$A_{\dot{x}} = K_{\dot{x}}\dot{x} + K_x \left(\frac{-T}{m} \right) \left[\frac{3}{\omega_o} - \frac{\omega_{ACVH}^2}{\omega_o^3} \right] \theta$$
$$+ K_x \left(\frac{-T}{m} \right) \left[\frac{K_{ACVH} \omega_{ACVH}^2}{\omega_o^3} \right] \delta + K_{\dot{x}} \left(\frac{-T}{m} \right) \left[\frac{3}{\omega_o^2} - \frac{2\zeta \omega_{ACVH}}{\omega_o^3} \right] \dot{\theta}$$

Appendix B: Engine Gimbaling Hover Cue Derivation

The derivation of hover cue control law with engine gimbaling for control is as follows.

The translational acceleration at the *cm* is:

$$\ddot{x} = \frac{-T}{m} \sin(\delta_q + \theta)$$

The Instantaneous Center-of-Rotation (ICR) position, l_{pitch} (i.e., ICR position relative to *cm*, positive down) is:

$$l_{pitch} = \frac{I_{yy}}{-\ell \cdot m}$$

where:

m is the vehicle mass

ℓ is the distance from the *cm* to the thrust application point

I_{yy} is the pitch inertia (in an aircraft body coordinate frame)

Velocity (\dot{x}) and acceleration (\ddot{x}) at ICR (assumes zero lateral offset (aircraft body X,Y axis) of gimbal from *cm*) follows from general equations:

$$\dot{x}_{ICR} = \dot{x}_{CM} + (\vec{\omega} \times \vec{r})$$

and

$$\ddot{x}_{ICR} = \ddot{x}_{CM} + (\vec{\omega} \times (\vec{\omega} \times \vec{r})) + (\dot{\vec{\omega}} \times \vec{r})$$

Yielding, for pitch/longitudinal axes only:

$$\dot{x}_{ICR} = \dot{x}_{cm} + q \cdot l_{pitch}$$

$$\ddot{x}_{ICR} = \ddot{x}_{cm} + \dot{q} \cdot l_{pitch} - p \cdot r \cdot l_{pitch}$$

It is assumed that the contribution of cross-coupling terms in acceleration will be negligible, that is:

$$\ddot{x}_{ICR} = \ddot{x}_{cm} + \dot{q} \cdot l_{pitch} - p \cdot r \cdot l_{pitch} = \ddot{x}_{cm} + \dot{q} \cdot l_{pitch}$$

For gimbaling control, the acceleration at the ICR is:

$$\ddot{x}_{ICR} = \frac{-T}{m} \sin(\delta_q + \theta) + \dot{q} \frac{I_{yy}}{-\ell \cdot m}$$

The hover cue control law from Eqn (2) is repeated here:

$$A_x = K_x \dot{x} + \frac{K_x \ddot{x}}{\omega_0^3} s(s^2 + 3\omega_0 s) + 3 \frac{K_x \ddot{x}}{\omega_0}$$

The hover cue is derived by substituting \ddot{x}_{ICR} in place of \ddot{x}_{CM} and \dot{x}_{ICR} in place of \dot{x}_{CM}

$$A_x = K_{\dot{x}}\dot{x}_{ICR} + \frac{K_{\dot{x}}}{\omega_0^3} \left(\frac{-T}{m} \sin(\delta_q + \theta) + \dot{q} \cdot \frac{I_{yy}}{-\ell \cdot m} \right) (s^2 + 3\omega_0 s) \\ + 3 \frac{K_{\dot{x}}}{\omega_0} \left(\frac{-T}{m} \sin(\delta_q + \theta) + \dot{q} \cdot \frac{I_{yy}}{-\ell \cdot m} \right)$$

It is assumed that $\sin(\delta_q + \theta) = \sin(\delta_q) + \sin(\theta)$:

$$A_x = K_{\dot{x}}\dot{x}_{ICR} + \frac{K_{\dot{x}}}{\omega_0^3} \left(\frac{-T}{m} (\sin(\delta_q) + \sin(\theta)) + \dot{q} \cdot \frac{I_{yy}}{-\ell \cdot m} \right) (s^2 + 3\omega_0 s) \\ + 3 \frac{K_{\dot{x}}}{\omega_0} \left(\frac{-T}{m} (\sin(\delta_q) + \sin(\theta)) + \dot{q} \cdot \frac{I_{yy}}{-\ell \cdot m} \right)$$

$$A_x = K_{\dot{x}}\dot{x}_{ICR} + \frac{K_{\dot{x}}}{\omega_0^3} \left(\frac{-T}{m} \sin(\delta_q) + \frac{-T}{m} \sin(\theta) + \dot{q} \cdot \frac{I_{yy}}{-\ell \cdot m} \right) (s^2 + 3\omega_0 s) \\ + 3 \frac{K_{\dot{x}}}{\omega_0} \left(\frac{-T}{m} \sin(\delta_q) + \frac{-T}{m} \sin(\theta) + \dot{q} \cdot \frac{I_{yy}}{-\ell \cdot m} \right)$$

Multiplying out $(s^2 + 3\omega_0 s)$ term:

$$A_x = K_{\dot{x}}\dot{x}_{ICR} + \frac{K_{\dot{x}}}{\omega_0^3} \left(\frac{-T}{m} \sin(\delta_q) s^2 + \frac{-T}{m} \sin(\theta) s^2 + \dot{q} \cdot \frac{I_{yy}}{-\ell \cdot m} s^2 \right) \\ + \frac{K_{\dot{x}}}{\omega_0^3} \left(\frac{-T}{m} \sin(\delta_q) 3\omega_0 s + \frac{-T}{m} \sin(\theta) 3\omega_0 s + \dot{q} \cdot \frac{I_{yy}}{-\ell \cdot m} 3\omega_0 s \right) \\ + 3 \frac{K_{\dot{x}}}{\omega_0} \left(\frac{-T}{m} \sin(\delta_q) + \frac{-T}{m} \sin(\theta) + \dot{q} \cdot \frac{I_{yy}}{-\ell \cdot m} \right)$$

It is assumed that the effects of the derivatives of $\sin(\delta_q)$ are negligible:

$$A_x = K_{\dot{x}}\dot{x}_{ICR} + \frac{K_{\dot{x}}}{\omega_0^3} \left(\frac{-T}{m} \sin(\theta) s^2 + \dot{q} \cdot \frac{I_{yy}}{-\ell \cdot m} s^2 \right) + \frac{K_{\dot{x}}}{\omega_0^3} \left(\frac{-T}{m} \sin(\theta) 3\omega_0 s + \dot{q} \cdot \frac{I_{yy}}{-\ell \cdot m} 3\omega_0 s \right) \\ + 3 \frac{K_{\dot{x}}}{\omega_0} \left(\frac{-T}{m} \sin(\delta_q) + \frac{-T}{m} \sin(\theta) + \dot{q} \cdot \frac{I_{yy}}{-\ell \cdot m} \right)$$

It is assumed that the effects of the first and second derivatives of \dot{q} are negligible and *assume* the first and second derivatives of $\sin(\theta)$ are equal to $\dot{\theta}$ and $\ddot{\theta}$, respectively:

$$A_x = K_{\dot{x}}\dot{x}_{ICR} + \frac{K_{\dot{x}}}{\omega_0^3} \left(\frac{-T}{m} \ddot{\theta} \right) + \frac{K_{\dot{x}}}{\omega_0^3} \left(\frac{-T}{m} 3\omega_0 \dot{\theta} \right) + 3 \frac{K_{\dot{x}}}{\omega_0} \left(\frac{-T}{m} \sin(\delta_q) + \frac{-T}{m} \sin(\theta) + \dot{\theta} \cdot \frac{I_{yy}}{-\ell \cdot m} \right)$$

Combining terms:

$$A_x = K_{\dot{x}}\dot{x}_{ICR} + \frac{K_{\dot{x}}}{\omega_0^3} \left(\frac{-T}{m} \ddot{\theta} \right) + 3 \frac{K_{\dot{x}}}{\omega_0} \frac{I_{yy}}{-\ell \cdot m} \dot{\theta} + \frac{K_{\dot{x}}}{\omega_0^3} \left(\frac{-T}{m} 3\omega_0 \right) \dot{\theta} \\ + 3 \frac{K_{\dot{x}}}{\omega_0} \left(\frac{-T}{m} \sin(\delta_q) + \frac{-T}{m} \sin(\theta) \right)$$

$$A_x = K_{\dot{x}} \dot{x}_{ICR} + \left(\frac{K_{\dot{x}}}{\omega_0^3} \left(\frac{-T}{m} \right) + 3 \frac{K_{\dot{x}}}{\omega_0} \frac{I_{yy}}{-\ell \cdot m} \right) \ddot{\theta} + \frac{K_{\dot{x}}}{\omega_0^3} \left(\frac{-T}{m} 3\omega_0 \right) \dot{\theta} + 3 \frac{K_{\dot{x}}}{\omega_0} \left(\frac{-T}{m} \sin(\delta_q) \right) + 3 \frac{K_{\dot{x}}}{\omega_0} \left(\frac{-T}{m} \sin(\theta) \right)$$

For gimbaled engine control:

$$\ddot{\theta} = - \left(\frac{T\ell}{I_{yy}} \right) \sin(\delta_q)$$

Substitute into the equation above

$$A_x = K_{\dot{x}} \dot{x}_{ICR} + \left(\frac{K_{\dot{x}}}{\omega_0^3} \left(\frac{-T}{m} \right) + 3 \frac{K_{\dot{x}}}{\omega_0} \frac{I_{yy}}{-\ell \cdot m} \right) \left(- \left(\frac{T\ell}{I_{yy}} \right) \sin(\delta_q) \right) + \frac{K_{\dot{x}}}{\omega_0^3} \left(\frac{-T}{m} 3\omega_0 \right) \dot{\theta} + 3 \frac{K_{\dot{x}}}{\omega_0} \left(\frac{-T}{m} \sin(\delta_q) \right) + 3 \frac{K_{\dot{x}}}{\omega_0} \left(\frac{-T}{m} \sin(\theta) \right)$$

$$A_x = K_{\dot{x}} \dot{x}_{ICR} + \left(\frac{K_{\dot{x}}}{\omega_0^3} \left(\frac{-T}{m} \right) \left(- \frac{T\ell}{I_{yy}} \right) + 3 \frac{K_{\dot{x}}}{\omega_0} \frac{I_{yy}}{-\ell \cdot m} \left(- \frac{T\ell}{I_{yy}} \right) \right) \sin(\delta_q) + \frac{K_{\dot{x}}}{\omega_0^3} \left(\frac{-T}{m} 3\omega_0 \right) \dot{\theta} + 3 \frac{K_{\dot{x}}}{\omega_0} \left(\frac{-T}{m} \sin(\delta_q) \right) + 3 \frac{K_{\dot{x}}}{\omega_0} \left(\frac{-T}{m} \sin(\theta) \right)$$

$$A_x = K_{\dot{x}} \dot{x}_{ICR} + \left(- \frac{K_{\dot{x}}}{\omega_0^3} \left(\frac{-T}{m} \right) \left(\frac{T\ell}{I_{yy}} \right) - 3 \frac{K_{\dot{x}}}{\omega_0} \left(\frac{-T}{m} \right) + 3 \frac{K_{\dot{x}}}{\omega_0} \left(\frac{-T}{m} \right) \right) \sin(\delta_q) + \frac{K_{\dot{x}}}{\omega_0^3} \left(\frac{-T}{m} 3\omega_0 \right) \dot{\theta} + 3 \frac{K_{\dot{x}}}{\omega_0} \left(\frac{-T}{m} \sin(\theta) \right)$$

The hover cue control law for engine gimbaling control becomes:

$$A_x = K_{\dot{x}} \dot{x}_{ICR} + \left(- \frac{K_{\dot{x}}}{\omega_0^3} \left(\frac{-T}{m} \right) \left(\frac{T\ell}{I_{yy}} \right) \right) \sin(\delta_q) + \frac{K_{\dot{x}}}{\omega_0^3} \left(\frac{-T}{m} 3\omega_0 \right) \dot{\theta} + 3 \frac{K_{\dot{x}}}{\omega_0} \left(\frac{-T}{m} \sin(\theta) \right)$$

For RCAH control law, we use the approximation that:

$$\frac{\dot{\theta}}{\delta} = \frac{K_{RCAH}}{(\tau_{RCAH} s + 1)}$$

$$\ddot{\theta} \tau_{RCAH} + \dot{\theta} = K_{RCAH} \delta$$

$$\dot{\theta} = K_{RCAH} \delta - \tau_{RCAH} \ddot{\theta}$$

For engine gimbaling control:

$$\dot{\theta} = K_{RCAH} \delta - \tau_{RCAH} \left(- \left(\frac{T\ell}{I_{yy}} \right) \sin(\delta_q) \right)$$

Substitute in Eqn (5):

$$A_x = K_{\dot{x}} \dot{x}_{ICR} + \left(-\frac{K_{\dot{x}}}{\omega_0^3} \left(\frac{-T}{m} \right) \left(\frac{T\ell}{I_{yy}} \right) \right) \sin(\delta_q) \\ + \frac{K_{\dot{x}}}{\omega_0^3} \left(\frac{-T}{m} 3\omega_0 \right) \left(K_{RCAH} \delta + \tau_{RCAH} \left(\frac{T\ell}{I_{yy}} \right) \sin(\delta_q) \right) + 3 \frac{K_{\dot{x}}}{\omega_0} \left(\frac{-T}{m} \sin(\theta) \right)$$

$$A_x = K_{\dot{x}} \dot{x}_{ICR} + \left(-\frac{K_{\dot{x}}}{\omega_0^3} \left(\frac{-T}{m} \right) \left(\frac{T\ell}{I_{yy}} \right) \right) \sin(\delta_q) + \frac{K_{\dot{x}}}{\omega_0^3} \left(\frac{-T}{m} 3\omega_0 \right) (K_{RCAH} \delta) \\ + \frac{K_{\dot{x}}}{\omega_0^3} \left(\frac{-T}{m} 3\omega_0 \right) \left(\tau_{RCAH} \left(\frac{T\ell}{I_{yy}} \right) \sin(\delta_q) \right) + 3 \frac{K_{\dot{x}}}{\omega_0} \left(\frac{-T}{m} \sin(\theta) \right)$$

$$A_x = K_{\dot{x}} \dot{x}_{ICR} + \left(-\frac{K_{\dot{x}}}{\omega_0^3} \left(\frac{-T}{m} \right) \left(\frac{T\ell}{I_{yy}} \right) + \frac{K_{\dot{x}}}{\omega_0^3} \left(\frac{-T}{m} 3\omega_0 \right) \left(\tau_{RCAH} \left(\frac{T\ell}{I_{yy}} \right) \right) \right) \sin(\delta_q) \\ + \frac{K_{\dot{x}}}{\omega_0^3} \left(\frac{-T}{m} 3\omega_0 \right) (K_{RCAH} \delta) + 3 \frac{K_{\dot{x}}}{\omega_0} \left(\frac{-T}{m} \sin(\theta) \right)$$

After clean up, the hover cue control law for a RCAH flight control system that employs engine gimbaling as the control effector is:

$$A_x = K_{\dot{x}} \dot{x}_{ICR} + \frac{K_{\dot{x}}}{\omega_0^3} \left(\frac{-T}{m} \right) \left(\frac{T\ell}{I_{yy}} \right) (3\omega_0(\tau_{RCAH}) - 1) \sin(\delta_q) + \frac{K_{\dot{x}}}{\omega_0^3} \left(\frac{-T}{m} 3\omega_0 \right) (K_{RCAH} \delta) \\ + 3 \frac{K_{\dot{x}}}{\omega_0} \left(\frac{-T}{m} \sin(\theta) \right)$$

The hover cue control law for a RCAH flight control system that employs engine gimbaling as the control effector, using cm reference, is:

$$A_x = K_{\dot{x}} (\dot{x}_{cm} + q \cdot l_{pitch}) + \frac{K_{\dot{x}}}{\omega_0^3} \left(\frac{-T}{m} \right) \left(\frac{T\ell}{I_{yy}} \right) (3\omega_0(\tau_{RCAH}) - 1) \sin(\delta_q) \\ + \frac{K_{\dot{x}}}{\omega_0^3} \left(\frac{-T}{m} 3\omega_0 \right) (K_{RCAH} \delta) + 3 \frac{K_{\dot{x}}}{\omega_0} \left(\frac{-T}{m} \sin(\theta) \right)$$